12-1-1990

The Hystery Unit - A Short Term Memory Model for Computational Neurons

M. D. Tom
Purdue University

M. F. Tenorio
Purdue University

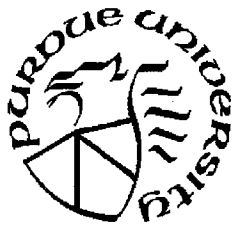

The Hystery Unit - A Short Term Memory Model for Computational Neurons

M. D. Tom
M. F. Tenorio

TR-EE 90-63
December, 1990

The Hystery Unit - A Short Term Memory Model for Computational Neurons

M. Daniel Tom

M. F. Tenorio

Parallel Distributed Structures Laboratory

School of Electrical Engineering

Purdue University

West Lafayette, Indiana 47907, USA

December, 1990

TR-EE 90-63

TABLE OF CONTENTS

The Hystery Unit - A Short Term Memory Model for Computational Neurons

M. Daniel Tom
M. F. Tenorio

Parallel Distributed Structures Laboratory
School of Electrical Engineering
Purdue University
West Lafayette, Indiana 47907, USA

December, 1990

Abstract

In this paper, a model of short term memory is introduced. This model is inspired by the transient behavior of neurons and magnetic storage as memory. The transient response of a neuron is hypothesized to be a combination of a pair of sigmoids, and a relation is drawn to the hysteresis loop characteristics of magnetic materials. A model is created as a composition of two coupled families of curves. Two theorems are derived regarding the asymptotic convergence behavior of the model. Another conjecture claims that the model retains full memory of all past unit step inputs.

Introduction

The sigmoid like graded response curve of a neuron used in neural computation research is often taken to be a scaled, displaced hyperbolic tangent. The graded response of the neuron (i.e. frequency of firing verses stimulus strength) to a stimulus is measured by probing neurons in a subject exposed to certain stimuli in a controlled environment.

However this response includes measurement error and the effect of the particular experimental methodology. Since the environment surrounding the neuron cannot be easily controlled, there are always stray stimuli that affect the measured response, and more importantly, the measurement methodology itself may be in question. Usually, the stimulus strength is chosen uniformly in a range between zero and that which produces saturation (highest frequency of firing). However the stimulus strength is not increased steadily from zero. Rather, the stimulus is varied slightly around a randomly chosen value for a short while before settling down to that value. Then a measurement of the frequency of firing is taken. Such randomization and jiggling of the stimulus are designed to overcome transient effects in the neural response. These transient effects can be easily experienced by the human eye. For example, after exposure to a photographic flash, the brightness impression on the retina persists for a few moments.

If the stimulus strength is steadily increased and decreased without randomization or jiggling, the neural response will likely follow two displaced hyperbolic tangent sigmoids, thus resembling a magnetic hysteresis loop. The fact that magnetic materials retain a magnetic field after an imposed electric field is removed is the basis of all magnetic storage devices. Thus short term memory, as a time-varying response of the neuron, is hypothesized to be akin to magnetic phenomena.

Short term memory is closely related to two types of simple, nonassociative learning — sensitization and habituation. Upon repeated or continued presentation of a stimulus, the intensity of the response of a nerve cell would either increase or fade away. The nerve cell adjusts to the environment by making plastic changes. When the stimulus is removed for some time, the nerve

cell recovers and the response intensity reverts to the normal level. The models to be developed below simulate some aspects of sensitization. With a sign change in one parameter, they become models for habituation.

The following sections present some of the early models developed for the study of short term memory. The Differential Equation Model, the Magnetization Model, and the hystery unit are closely related to one another. The Magnetization Model is developed to simulate hysteresis loops and the magnetization curve of magnetic materials. The hystery unit eliminates the use of a description of the magnetization curve. Its output converges to the hysteresis loops asymptotically. Upon differentiation of the model equations, it is found that the hystery unit is identical to the Differential Equation Model unit.

Two theorems and proofs describe and support the asymptotic convergence property observed in the hystery unit's output. The hystery unit is also observed to give distinct outputs for different input sequences of unit steps. The step size modulates the distribution of the final outputs. Different outputs appear to be sorted, and is analyzed in one of the following sections. Lastly the hystery unit is applied to a spatiotemporal pattern recognition problem. Its nonlinear memory characteristics give some interesting results.

Model 0: Time Delay Model

Lissajous Figures are obtained on the screen of an oscilloscope when the x-input is driven by a periodic waveform, and the y-input is driven by the magnetic field response of a magnetic material to the electric field imposed. For some magnetic materials, the figure is an ellipse, showing that the output is merely a delayed and scaled version of the input. The Time Delay Model below incorporates both delay and nonlinear characteristics:

$$y(t) = S(x(t - \Delta t)), \text{ where} \tag{1}$$

$$S(x) = \tanh x \tag{2}$$

Model 1: Differential Equation Model

The Differential Equation Model assumes that the rate of change of the response, instead of the response itself, follows a sigmoid. To achieve the saturation effect, a gating multiplier is employed. This combination produces the following:

$$\frac{dy}{dx} = (1 - y)\ S(x), \text{ where} \tag{3}$$

$$S(x) = 1 + \tanh\ (x - H_c) = \frac{2}{1 + e^{-2(x-H_c)}} \tag{4}$$

This differential equation is appropriate for $\Delta x > 0$. For $\Delta x < 0$, the following differential equation is used:

$$\frac{dy}{dx} = (1 + y)\ S(-x) \tag{5}$$

Model 2: Exponential Model

The nonlinearity of the Exponential Model distinguishes it from the Differential Equation Model. Instead of the hyperbolic tangent sigmoid, the exponential function is used. For $\Delta x > 0$,

$$\frac{dy}{dx} = (1 - y)\ S(x), \text{ where} \tag{6}$$

$$S(x) = \exp\ (x - H_c) \tag{7}$$

For $\Delta x < 0$,

$$\frac{dy}{dx} = (1 + y)\ S(-x) \tag{8}$$

For simplicity's sake, the solution to $\frac{dy}{dx} = (1 - y)\ S(x)$ for $\Delta x > 0$ is called the rising curve. The falling curve will designate the solution to $\frac{dy}{dx} = (1 + y)\ S(-x)$ for $\Delta x < 0$.

This model is different from the Differential Equation Model in that the rising curve is unlike the hyperbolic tangent; it rises gently, but saturates

sharply.

Model 3: Magnetization Model

In order to capture the magnetic hysteresis loop effect, the magnetization model is created. First, it is assumed that the upper and lower branches of the hysteresis loop are both hyperbolic tangent functions. Second, it is assumed that the displacement of these functions along the x-axis is H_c (modeled after the coercive magnetic field required to bring the magnetic field in magnetic materials to zero). Here H_c is taken as a magnitude, and is thus a positive quantity.

To accommodate any starting point in the x,y-plane, the lower and upper branches of the hysteresis loop are actually described as two families of curves. When x is increasing, a rising curve is followed, causing the output y to increase with x. As soon as x starts decreasing, a falling curve is traced, causing the output y to decay with x. The set of rising curves that passes through all possible starting points forms the family of rising curves (see Figure 1). Each member, indexed by η, has the form:

$$y = \eta + (1 - \eta) \tanh (x - H_c) \tag{9}$$

for some η satisfying

$$y_0 = \eta + (1 - \eta) \tanh (x_0 - H_c) \tag{10}$$

with (x_0, y_0) being a point where the curve passes through, where $x_0 < x$. Solving for η,

$$\eta = \frac{y_0 - \tanh (x_0 - H_c)}{1 - \tanh (x_0 - H_c)} \tag{11}$$

For the case where $x_0 > x$, the family of falling curves is (see Figure 2):

$$y = -\eta + (1 - \eta) \tanh (x + H_c), \text{ and} \tag{12}$$

$$\eta = \frac{y_0 - \tanh (x_0 + H_c)}{-1 - \tanh (x_0 + H_c)} \tag{13}$$

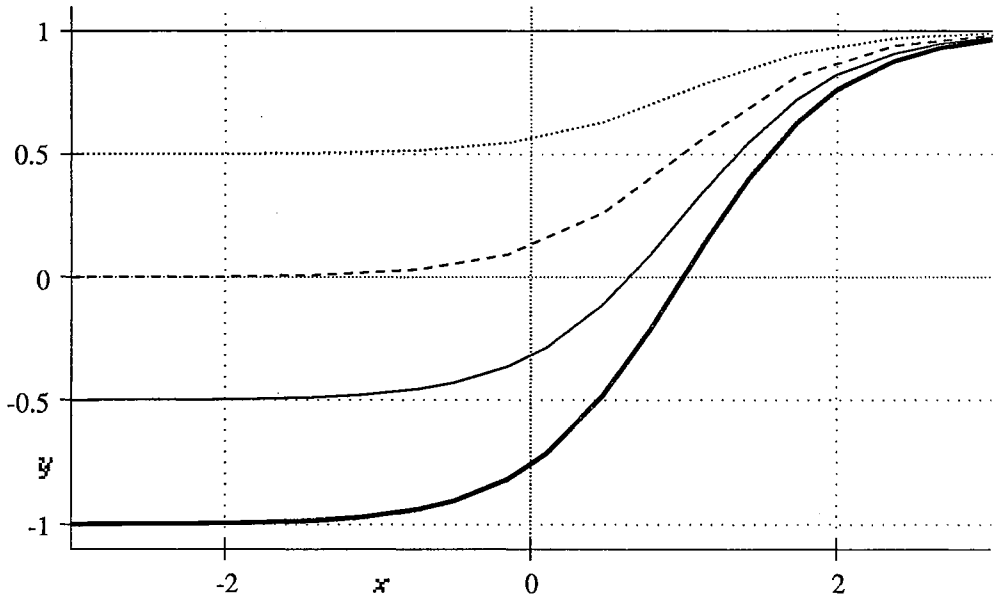

Figure 1. Five members of the family of rising curves. The thick line, solid line, dashed line, dotted line, and the solid line from bottom to top represent members with indices 0, 0.25, 0.5, 0.75, and 1 respectively.

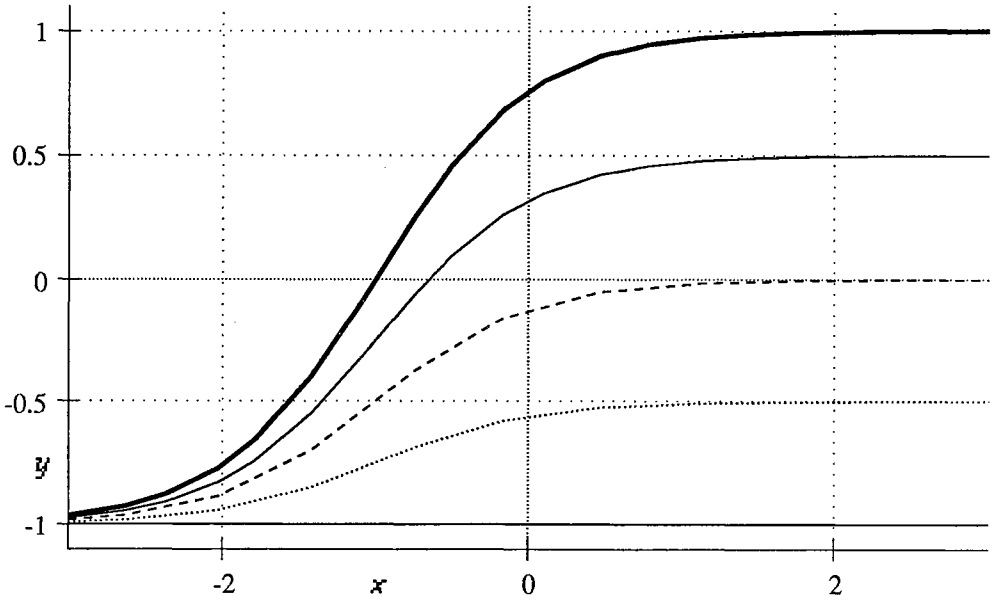

Figure 2. Five members of the family of falling curves. The thick line, solid line, dashed line, dotted line, and the solid line from top to bottom represent members with indices 0, 0.25, 0.5, 0.75, and 1 respectively.

Thus, the index η controls the vertical displacement as well as the compression of the hyperbolic tangent nonlinearity. To allow for saturations other than unity, a scaling factor can be incorporated into the family:

$$y = B_s[\eta + (1 - \eta) \tanh (x - H_c)] \tag{14}$$

In this case, the output value has to be rescaled in the computation of η:

$$\eta = \frac{(y_0/B_s) - \tanh (x_0 - H_c)}{1 - \tanh (x_0 - H_c)} \tag{15}$$

For the most part, the scaling multiplier B_s will be left out of the discussion that follows. The displacement factor H_c will be retained instead.

The Magnetization Curve

There is a third assumption that the magnetization curve which passes through the origin is the locus of the intersection points of the upper and lower branches of the loop as η varies. The two families can be renamed for clarification as follows. The family of rising curves is:

$$y^+ = \eta^+ + (1 - \eta^+) \tanh (x - H_c) \tag{16}$$

$$\eta^+ = \frac{y_0 - \tanh (x_0 - H_c)}{1 - \tanh (x_0 - H_c)} \tag{17}$$

The family of falling curves is:

$$y^- = \eta^- + (1 - \eta^-) \tanh (x + H_c) \tag{18}$$

$$\eta^- = \frac{y_0 - \tanh (x_0 + H_c)}{-1 - \tanh (x_0 + H_c)} \tag{19}$$

To solve for the magnetization curve (the curve that starts from the origin), the quantities y^+ and y^- are equated, and since $\eta^+ = \eta^- = \eta$ by symmetry:

$$\eta + (1 - \eta) \tanh (x - H_c) = -\eta + (1 - \eta) \tanh (x + H_c) \tag{20}$$

$$2\eta = (1 - \eta)[\tanh (x + H_c) - \tanh (x - H_c)] \tag{21}$$

Note that

$$\tanh(x+H_c)-\tanh(x-H_c)=\frac{e^{x+H_c}-e^{-x-H_c}}{e^{x+H_c}+e^{-x-H_c}}-\frac{e^{x-H_c}-e^{-x+H_c}}{e^{x-H_c}+e^{-x+H_c}}$$

$$=\frac{e^{2H_c}+e^{-2x}-e^{2x}-e^{-2H_c}+e^{2H_c}+e^{2x}-e^{-2x}-e^{-2H_c}}{e^{2H_c}+e^{-2x}+e^{2x}+e^{-2H_c}}$$

$$=\frac{2\left(e^{2H_c}-e^{-2H_c}\right)}{e^{2H_c}+e^{-2x}+e^{2x}+e^{-2H_c}}$$

$$=\frac{2\sinh 2H_c}{\cosh 2x+\cosh 2H_c} \tag{22}$$

Therefore,

$$\frac{2\eta}{1-\eta}=\frac{2\sinh 2H_c}{\cosh 2x+\cosh 2H_c}$$

$$\eta(\cosh 2x+\cosh 2H_c)=\sinh 2H_c-\eta\sinh 2H_c$$

$$\eta=\frac{\sinh 2H_c}{\cosh 2x+\cosh 2H_c+\sinh 2H_c}$$

$$\eta=\frac{\sinh 2H_c}{\cosh 2x+\exp(2H_c)} \tag{23}$$

Substituting η into either family, the magnetization curve is obtained:

$$y=\tanh(x-H_c)+[1-\tanh(x-H_c)]\frac{\sinh 2H_c}{\cosh 2x+\exp(2H_c)}$$

$$=\frac{(\cosh 2x+\cosh 2H_c)\tanh(x-H_c)+\sinh 2H_c}{\cosh 2x+\cosh 2H_c+\sinh 2H_c} \tag{24}$$

The magnetization curve is symmetric about the origin. To show this, first denote y by y^+. Let y^- be the expression for y with $-x$ substituted for x. That is,

$$y^-=\frac{(\cosh -2x+\cosh 2H_c)\tanh(-x-H_c)+\sinh 2H_c}{\cosh -2x+\cosh 2H_c+\sinh 2H_c} \tag{25}$$

Since $\cosh -2x=\cosh 2x$,

$$y^-=\frac{(\cosh 2x+\cosh 2H_c)\tanh(-x-H_c)+\sinh 2H_c}{\cosh 2x+\cosh 2H_c+\sinh 2H_c} \tag{26}$$

Now add y^+ and y^-. The numerator is:

$$\begin{aligned}
&(\cosh -2x + \cosh 2H_c)[\tanh (x - H_c) + \tanh (-x - H_c)] + 2\sinh 2H_c \\
&= (\cosh -2x + \cosh 2H_c)[\tanh (x - H_c) - \tanh (x + H_c)] + 2\sinh 2H_c \\
&= (\cosh -2x + \cosh 2H_c)\left[\frac{-2\sinh 2H_c}{\cosh -2x + \cosh 2H_c}\right] + 2\sinh 2H_c \\
&= 0 \qquad (27)
\end{aligned}$$

Therefore, $y^+ = -y^-$. The magnetization curve thus has odd symmetry about the origin.

Measures of Memory

As mentioned above, one of the characteristics of magnetic hysteresis is the presence of a residual magnetic field after the imposed electric field is removed. One interesting question is, after driving the model with some units of input, how many units of reverse input are required to bring the output to the "knee" of the nonlinearity? Specifically, the "knee" of the nonlinearity is the transition between saturation and the almost-linear part in the middle. The exact location of this transition of the hyperbolic tangent will be defined as the place where the third derivative is zero, which is computed below:

$$y = \tanh x = \frac{\sinh x}{\cosh x} \qquad (28)$$

$$\begin{aligned}
y' &= \frac{\cosh^2 x - \sinh^2 x}{\cosh^2 x} \\
&= 1 - \tanh^2 x \\
&= 1 - y^2 \qquad (29)
\end{aligned}$$

$$\begin{aligned}
y'' &= -2y\,y' \\
&= -2\tanh x\,(1 - \tanh^2 x) \\
&= 2y^3 - 2y \qquad (30)
\end{aligned}$$

$$\begin{aligned}
y''' &= (6y^2 - 2)y' \\
&= 2(3y^2 - 1)(1 - y^2) \qquad (31)
\end{aligned}$$

Setting $y''' = 0$ would imply $3 \tanh^2 x = 1$, since $|\tanh x| < 1$. This gives $x = \tanh^{-1}(1/\sqrt{3})$ as the point of interest. Suppose a units of input are applied, starting from the origin. This brings the model along the magnetization curve to $x = a$. To bring the output to the transition between saturation and linearity, the input has to be driven reversely to this transition point of hyperbolic tangent, now a member in the family of falling curves. As this transition depends only on the horizontal displacement H_c, but not vertical scaling, its location along the x-axis is thus independent of the member in the family. Therefore, starting from the point where the $x = a$, a reverse input of magnitude $a + H_c - \tanh^{-1}(1/\sqrt{3})$ is required. (Figure 3, solid line.)

Another good measure of the retentivity property of Model 3 is the amount of reverse input required to drive the output to zero given some amount of positive input has applied to the model starting from the origin. The amount of reverse input will be dependent on the magnitude of the forward input. Different magnitudes of forward input will bring the output to different points on the magnetization curve. Different reverse traces on different members of the family of falling curves will be produced. The x-intersection of the member given a forward input of a units is derived below.

Remember the magnetization curve is defined as the locus of the intersection of two members, one from each family, that have the same displacement and scaling factor η. Thus, having driven Model 3 from origin with a forward input of magnitude a, the output falls on the magnetization curve where

$$\eta = \frac{\sinh 2H_c}{\cosh 2a + \cosh 2H_c + \sinh 2H_c} \tag{32}$$

The member of the family of falling curves will have this index η. The falling curve is:

$$y = -\eta + (1 - \eta) \tanh (x + H_c) \tag{33}$$

As the x-intersection is of interest, set $y = 0$. Then

$$\tanh (x + H_c) = \frac{\eta}{1 - \eta}$$

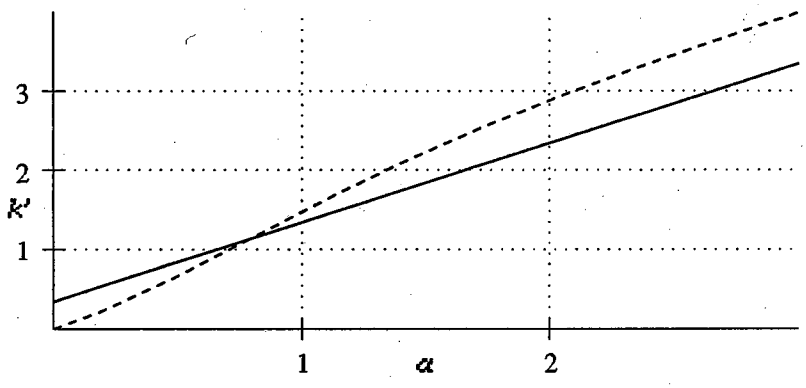

Figure 3. Measures of memory: The solid line shows the reverse input required to bring the output of Model 3 to the transition between the saturation region and the linear region, given the forward input is a and Hc = 1. The dashed line shows the reverse input required to bring the output to zero.

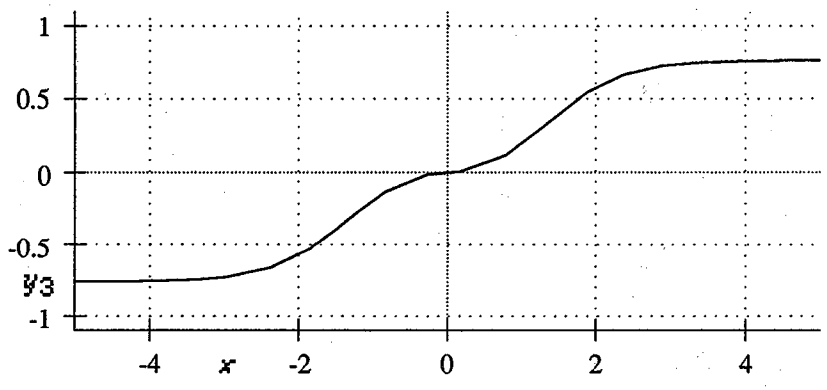

Figure 4. Residual memory: The graph shows the residual output of Model 3 when the input is reduced to zero after an input x is applied.

$$\tanh\,(x + H_c) = \frac{\sinh 2H_c}{\cosh 2a + \cosh 2H_c}$$

$$x = -H_c + \tanh^{-1}\left(\frac{\sinh 2H_c}{\cosh 2a + \cosh 2H_c}\right) \tag{34}$$

The reverse input required to bring the output to zero is therefore (Figure 3, dashed line):

$$a + H_c - \tanh^{-1}\left(\frac{\sinh 2H_c}{\cosh 2a + \cosh 2H_c}\right) \tag{35}$$

Yet a third measure of the memory of the model is the parallel of residual flux in magnetic materials. In Model 3, the residual left behind after an input of magnitude a is applied is the y-crossing of the falling curve. (Figure 4.) Setting $x = 0$,

$$y = -\eta + (1 - \eta)\tanh H_c \tag{36}$$

Substituting η from above,

$$y = \frac{-\sinh 2H_c + (\cosh 2a + \cosh 2H_c)\tanh H_c}{\cosh 2a + \cosh 2H_c + \sinh 2H_c} \tag{37}$$

Note its similarity and differences with the magnetization curve:

$$y = \frac{(\cosh 2x + \cosh 2H_c)\tanh (x - H_c) + \sinh 2H_c}{\cosh 2x + \cosh 2H_c + \sinh 2H_c} \tag{38}$$

Model 4: The Hystery Unit

The magnetization curve of Model 3 provides immediate access to the hysteresis loop effect upon an a.c. input. However, the magnetization curve becomes an extra condition imposed on the input that start from the origin. To ease this restriction, Model 4, called the hystery unit, is created without the magnetization curve assumption. The "magnetization curve" will be just one member in the family of rising curves and another in the family of falling curves that pass through the origin. (Figure 5.) For $x > 0$, this curve is:

$$y = \eta + (1 - \eta)\tanh (x - H_c) \tag{39}$$

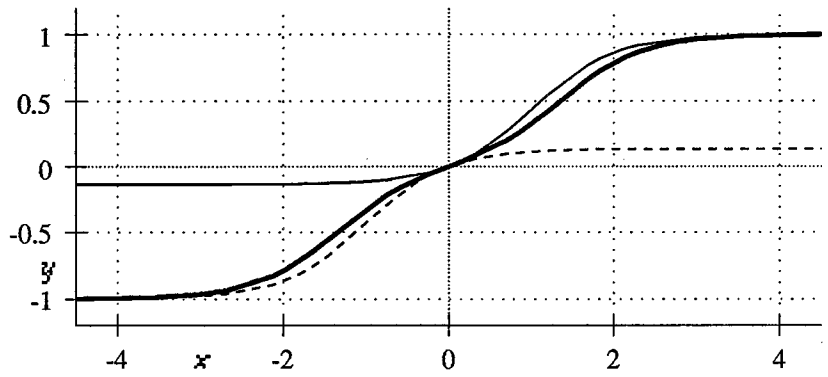

Figure 5. Magnetization curves: The heavy line shows the magnetization curve used in Model 3. The solid line and the dashed line show respectively the rising curve and falling curve of Model 4 which pass through the origin.

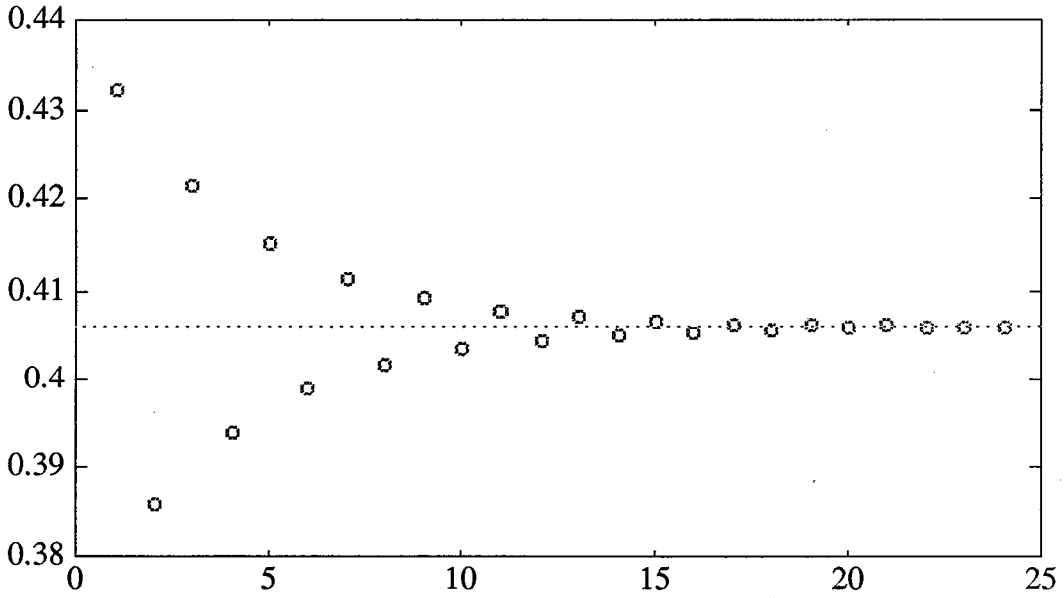

Figure 6. Convergence of the index into the family of curves under no bias. The a.c. magnitude is 0.5; Bs = 1; Hc = 1; starting from (0,0).

where η is now specifically:

$$\eta_{(0,0)} = \frac{0 - \tanh(0 - H_c)}{1 - \tanh(0 - H_c)}$$

$$= \frac{\tanh H_c}{1 + \tanh H_c} \tag{40}$$

The "magnetization curve" thus reduces to:

$$y = \frac{\tanh(x - H_c) + \tanh H_c}{1 + \tanh H_c} \tag{41}$$

Similarly, for $x < 0$,

$$y = \frac{\tanh(x + H_c) - \tanh H_c}{1 + \tanh H_c} \tag{42}$$

With this new change, the model is simplified. However, the looping effect is not observed immediately upon an a.c. input. It is observed that given steady a.c. input, the output asymptotically converges to a loop which is identical to the loop obtained in Model 3. Two theorems and proofs below establish this asymptotic convergence property. Moreover, it is observed that different sequences of unit step inputs result in different outputs. Thus given an output, there is only one sequence of stepwise input that can drive the model from rest to the particular output. The hystery unit therefore has full memory of the history of inputs.

> Theorem 1: Hysteresis is a steady state behavior of the hystery unit under constant magnitude a.c. input.
>
> Theorem 2: η_k converges to $(\sinh 2H_c) / [\cosh 2a + \exp(2H_c)]$, where η_k denotes the successive indices of the members of the two families of curves followed under unbiased a.c. input.

When the input increases, the output of the hystery unit follows one member of the family of rising curves. Similarly when the input decreases, the output of the hystery unit follows one member of the family of falling curves. Therefore in one cycle of a.c. input from the negative peak to the positive peak,

and to the negative peak, only one member of each family of curves is followed. It is therefore convenient only to consider the convergence of the indices.

Proof of Theorem 2

The proof will consist of three parts. The first part is to find the limit η to which η_k converges. The second part is to show that $\{\eta_k\}$ is a sequence that oscillates about η. The third part is to show that if $\eta_1 > \eta$, then $\eta_{2k+1} < \eta_{2k-1}$, and $\eta_{2k+2} > \eta_{2k}$.

Assume $\lim_{k\to\infty} \eta_k = \eta$. Then $\lim_{k\to\infty} \eta_{2k} = \eta$, and $\lim_{k\to\infty} \eta_{2k+1} = \eta$. Without loss of generality, assume $\eta_1 = \dfrac{y_0 - \tanh(x_0 - H_c)}{1 - \tanh(x_0 - H_c)}$, and the a.c. input driving the hystery unit has a magnitude of a.

$$\eta_{2k+1} = \frac{y_{2k} - \tanh(-a - H_c)}{1 - \tanh(-a - H_c)}$$

$$= \frac{-\eta_{2k} + (1 - \eta_{2k}) \tanh(-a + H_c) + \tanh(a + H_c)}{1 + \tanh(a + H_c)} \tag{43}$$

Taking the limit as k approaches infinity on both sides,

$$\eta = \frac{-\eta + (1 - \eta) \tanh(-a + H_c) + \tanh(a + H_c)}{1 + \tanh(a + H_c)}$$

$$\eta\,[1 + \tanh(a + H_c)] = -\eta + (1 - \eta) \tanh(-a + H_c) + \tanh(a + H_c)$$

$$\eta\,[2 + \tanh(a + H_c) + \tanh(-a + H_c)] = \tanh(a + H_c) + \tanh(-a + H_c)$$

$$\eta\,[2 + \tanh(a + H_c) - \tanh(a - H_c)] = \tanh(a + H_c) - \tanh(a - H_c)$$

$$\eta = \frac{\tanh(a + H_c) - \tanh(a - H_c)}{2 + \tanh(a + H_c) - \tanh(a - H_c)} \tag{44}$$

As derived earlier,

$$\tanh(a + H_c) - \tanh(a - H_c) = \frac{2 \sinh 2H_c}{\cosh 2a + \cosh 2H_c} \tag{45}$$

Therefore,

$$\eta = \frac{2 \sinh 2H_c \,/\, (\cosh 2a + \cosh 2H_c)}{2 + 2 \sinh 2H_c \,/\, (\cosh 2a + \cosh 2H_c)}$$

$$= \frac{\sinh 2H_c}{\cosh 2a + \cosh 2H_c + \sinh 2H_c}$$

$$= \frac{\sinh 2H_c}{\cosh 2a + e^{2H_c}} \tag{46}$$

To show that $\{\eta_k\}$ is an oscillation sequence, consider Equation 43 above:

$$\eta_{2k+1} = \frac{-\eta_{2k} + (1 - \eta_{2k}) \tanh (-a + H_c) + \tanh (a + H_c)}{1 + \tanh (a + H_c)}$$

$$= \frac{\tanh (a + H_c) - \tanh (a - H_c) - [1 - \tanh (a - H_c)]\, \eta_{2k}}{1 + \tanh (a + H_c)}$$

Alternatively, from the definitions,

$$\eta_{2k} = \frac{y_{2k-1} - \tanh (a + H_c)}{-1 - \tanh (a + H_c)}$$

$$= \frac{-y_{2k-1} + \tanh (a + H_c)}{1 + \tanh (a + H_c)}$$

$$= \frac{-\eta_{2k-1} - (1 - \eta_{2k-1}) \tanh (a - H_c) + \tanh (a + H_c)}{1 + \tanh (a + H_c)}$$

$$= \frac{\tanh (a + H_c) - \tanh (a - H_c) - [1 - \tanh (a - H_c)]\, \eta_{2k-1}}{1 + \tanh (a + H_c)} \tag{47}$$

Thus both η_{2k+1} and η_{2k} can be expressed in the common form below:

$$\eta_{k+1} = \frac{\tanh (a + H_c) - \tanh (a - H_c) - [1 - \tanh (a - H_c)]\, \eta_k}{1 + \tanh (a + H_c)} \tag{48}$$

If $\eta_{k+1} < \eta$,

$$\eta > \frac{\tanh (a + H_c) - \tanh (a - H_c) - [1 - \tanh (a - H_c)]\, \eta_k}{1 + \tanh (a + H_c)}$$

$$\eta_k > \frac{\tanh (a + H_c) - \tanh (a - H_c) - [1 + \tanh (a + H_c)]\, \eta}{1 - \tanh (a - H_c)} \tag{49}$$

Let $\gamma = \tanh(a + H_c) - \tanh(a - H_c)$. From Equation 44 above,

$$\eta = \frac{\gamma}{2 + \gamma} \tag{50}$$

$$2\eta + \gamma\eta = \gamma$$

$$2\eta = \gamma(1 - \eta)$$

$$\gamma = \frac{2\eta}{1 - \eta} \tag{51}$$

Also, since $\gamma = \tanh(a + H_c) - \tanh(a - H_c)$,

$$\begin{aligned} 1 - \tanh(a - H_c) &= 1 + \gamma - \tanh(a + H_c) \\ &= 1 + \frac{2\eta}{1 - \eta} - \tanh(a + H_c) \end{aligned} \tag{52}$$

Continuing, we have

$$\begin{aligned} \eta_k &> \frac{\frac{2\eta}{1 - \eta} - [1 + \tanh(a + H_c)]\,\eta}{1 + \frac{2\eta}{1 - \eta} - \tanh(a + H_c)} \\ &= \frac{2\eta - \eta(1 - \eta)[1 + \tanh(a + H_c)]}{1 - \eta + 2\eta - (1 - \eta)\tanh(a + H_c)} \\ &= \frac{2\eta - \eta(1 - \eta)[1 + \tanh(a + H_c)]}{1 + \eta - (1 - \eta)\tanh(a + H_c)} \\ &= \frac{2\eta - \eta(1 - \eta)[1 + \tanh(a + H_c)]}{1 + \eta + (1 - \eta) - (1 - \eta)[1 + \tanh(a + H_c)]} \\ &= \frac{\eta\{2 - (1 - \eta)[1 + \tanh(a + H_c)]\}}{2 - (1 - \eta)[1 + \tanh(a + H_c)]} \\ &= \eta \end{aligned} \tag{53}$$

Otherwise, if $\eta_{k+1} > \eta$, then $\eta_k < \eta$. Thus the sequence $\{\eta_k\}$ is oscillating about η.

The last part of the proof is to show that η_{2k} and η_{2k+1} are monotonically increasing and decreasing, or vice versa. From Equation 48 above, increasing the index by one,

$$\eta_{k+2} = \frac{\tanh(a + H_c) - \tanh(a - H_c) - [1 - \tanh(a - H_c)]\,\eta_{k+1}}{1 + \tanh(a + H_c)} \tag{54}$$

Using the previous shorthand notation γ, and let $T = \tanh(a + H_c)$,

$$\begin{aligned}
\eta_{k+2} &= \frac{1}{1+T}\left[\gamma - (1 - T + \gamma)\,\eta_{k+1}\right] \\
&= \frac{1}{1+T}\left\{\gamma - \frac{1 - T + \gamma}{1+T}\left[\gamma - (1 - T + \gamma)\,\eta_k\right]\right\} \\
&= \frac{1}{1+T}\left\{\gamma - \gamma\,\frac{1 - T + \gamma}{1+T} + \frac{(1 - T + \gamma)^2}{1+T}\,\eta_k\right\} \\
&= \frac{\gamma(1 + T - 1 + T - \gamma) + (1 - T + \gamma)^2\eta_k}{(1+T)^2}
\end{aligned} \tag{55}$$

$$\begin{aligned}
\eta_{k+2} - \eta_k &= \frac{\gamma(2T - \gamma) + [(1 - T + \gamma)^2 - (1+T)^2]\,\eta_k}{(1+T)^2} \\
&= \frac{\gamma(2T - \gamma) + (\gamma^2 + 2\gamma - 2\gamma T - 4T)\,\eta_k}{(1+T)^2} \\
&= \frac{\gamma(2T - \gamma) + [\gamma(\gamma - 2T) + 2(\gamma - 2T)]\,\eta_k}{(1+T)^2} \\
&= \frac{2T - \gamma}{(1+T)^2}\left[\gamma - (\gamma + 2)\,\eta_k\right]
\end{aligned} \tag{56}$$

Since $T = \tanh(a + H_c) > -1$, so $(1 + T)^2 > 0$, and

$$\begin{aligned}
2T - \gamma &= \tanh(a + H_c) + \tanh(a - H_c) \\
&= \frac{2 \sinh 2a}{\cosh 2a + \cosh 2H_c} \\
&> 0 \text{ since } a > 0.
\end{aligned} \tag{57}$$

If $\gamma - (\gamma + 2)\,\eta_k < 0$, or equivalently, $\eta_k > \dfrac{\gamma}{2 + \gamma} = \eta$, then $\eta_{k+2} < \eta_k$, and the sequence is monotonically decreasing. Conversely, if $\eta_k < \eta$, then $\eta_{k+2} > \eta_k$, and the sequence is monotonically increasing. Following the assumption that $\eta_1 = \dfrac{y_0 - \tanh(x_0 - H_c)}{1 - \tanh(x_0 - H_c)} > 0$, the sequence $\{\eta_1, \eta_3, \eta_5, \cdots\}$

is monotonically decreasing with all terms greater than η, and thus converges to η. Similarly, the sequence $\{\eta_2, \eta_4, \eta_6, \cdots\}$ is monotonically increasing with all terms less than η, and therefore also converges to η. (Figure 6.)

Now Theorem 2 is proved independent of a, the magnitude of the a.c. input (Figure 7), and (x_0, y_0), the starting point before applying the a.c. input. It is therefore possible to start at some point outside the realm of magnetic hysteresis loops. (See Figures 8-12.)

Proof of Theorem 1

Theorem 1 is a generalization of Theorem 2, stating that a.c. input with d.c. bias can also make the hystery unit converge to steady state. The proof of Theorem 1 will be different from that of Theorem 2. This proof is divided into two parallel parts outlined as follows. The first half is to prove that the sequence $\{\eta_k^+\}$ converges to η^+. To prove this, first the limit η^+ to which $\{\eta_k^+\}$ converges is found. Then $\eta_k^+ > \eta^+$ for all k (or $\eta_k^+ < \eta^+$ for all k) is established. Finally, the proof that η_k^+ is monotonically decreasing (or increasing) completes the proof of the first half of Theorem 2. The second half is to prove that the sequence $\{\eta_k^-\}$ converges to η^-, using a similar approach.

As mentioned above, the set of equations for the families of rising and falling curves may be renamed more clearly as follows:

$$y_k^+ = \eta_k^+ + (1 - \eta_k^+) \tanh (x_k^+ - H_c), \text{ where}$$

$$\eta_k^+ = \frac{y_{k-1}^- - \tanh (x_{k-1}^- - H_c)}{1 - \tanh (x_{k-1}^- - H_c)} \tag{58}$$

$$y_k^- = -\eta_k^- + (1 - \eta_k^-) \tanh (x_k^- + H_c), \text{ where}$$

$$\eta_k^- = \frac{y_k^+ - \tanh (x_k^+ + H_c)}{-1 - \tanh (x_k^+ + H_c)} \tag{59}$$

Without loss of generality, let $x_k^+ = b + a$, and $x_k^- = b - a$. It will be convenient to use the following shorthand notations:

$$T_1 = \tanh (b - a - H_c); \quad S_1 = \sinh (b - a - H_c); \quad C_1 = \cosh (b - a - H_c)$$

$$T_2 = \tanh (b - a + H_c); \quad S_2 = \sinh (b - a + H_c); \quad C_2 = \cosh (b - a + H_c)$$

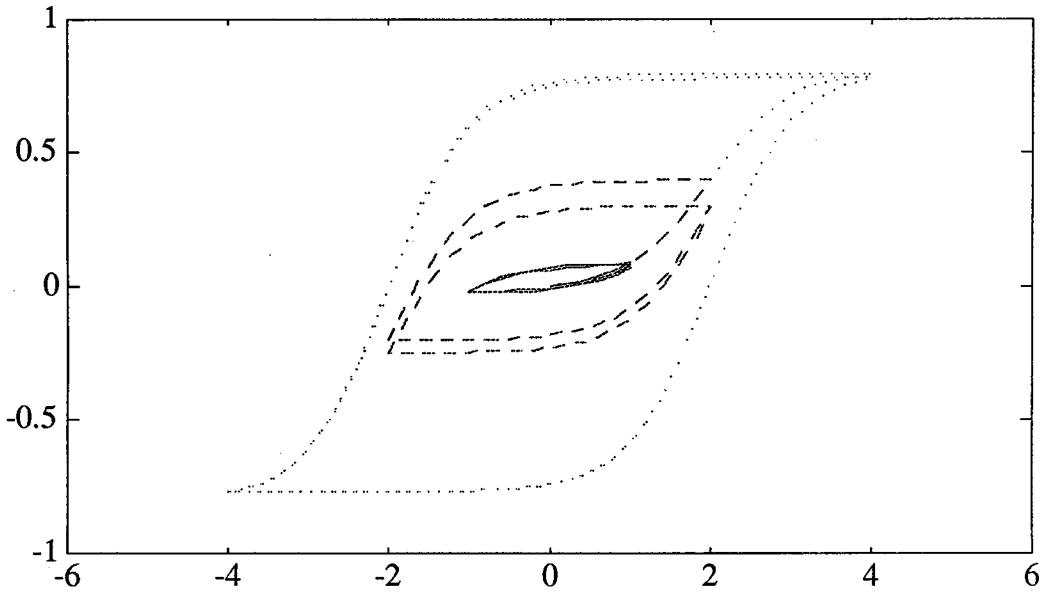

Figure 7. Convergence of the hystery unit under various a.c. input magnitudes. The solid line, dashed line, and dotted line represent responds to a.c input of magnitudes 1, 2, and 4 respectively. Bs = 0.8; Hc = 2.

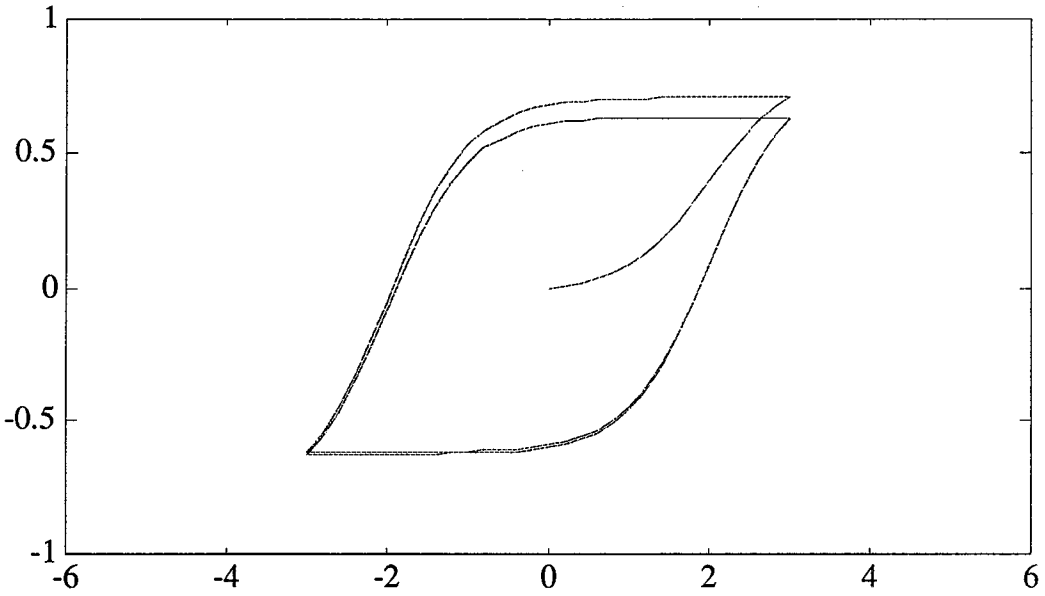

Figure 8. Convergence of the hystery unit when driven from (0,0). The amplitude of the a.c. input is 3; Bs = 0.8; Hc = 2.

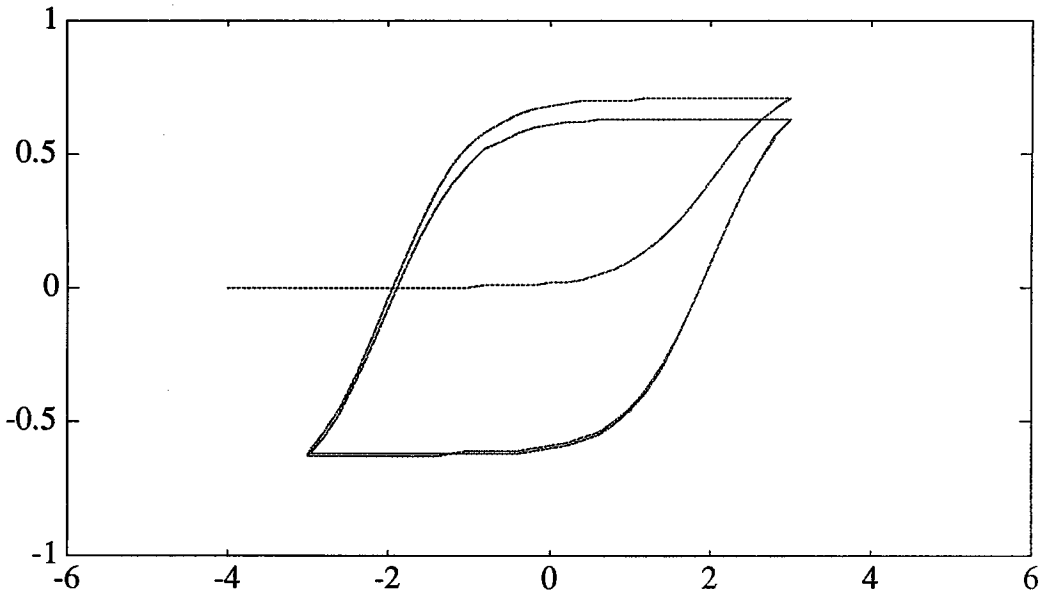

Figure 9. Convergence of the hystery unit when driven from (-4,0).
The amplitude of the a.c. input is 3; Bs = 0.8; Hc = 2.

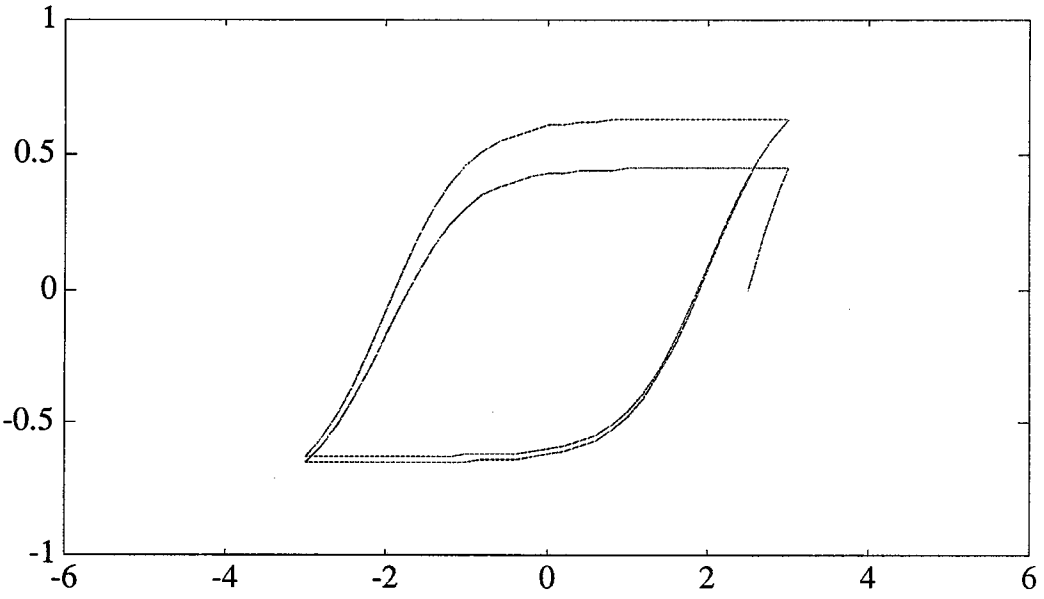

Figure 10. Convergence of the hystery unit when driven from (2.5,0).
The amplitude of the a.c. input is 3; Bs = 0.8; Hc = 2.

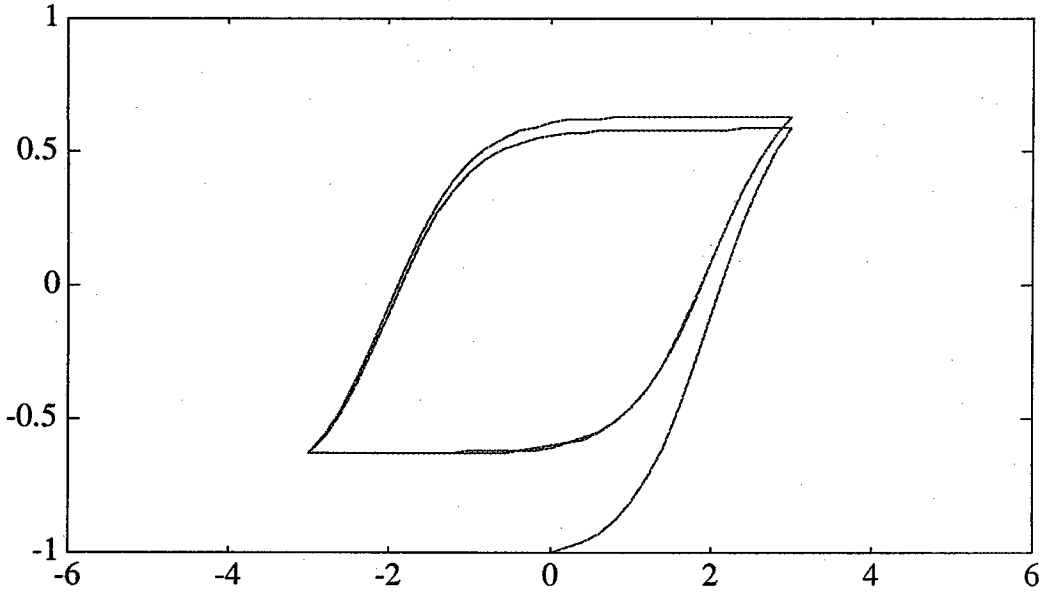

Figure 11. Convergence of the hystery unit when driven from (0,-1).
The amplitude of the a.c. input is 3; Bs = 0.8; Hc = 2.

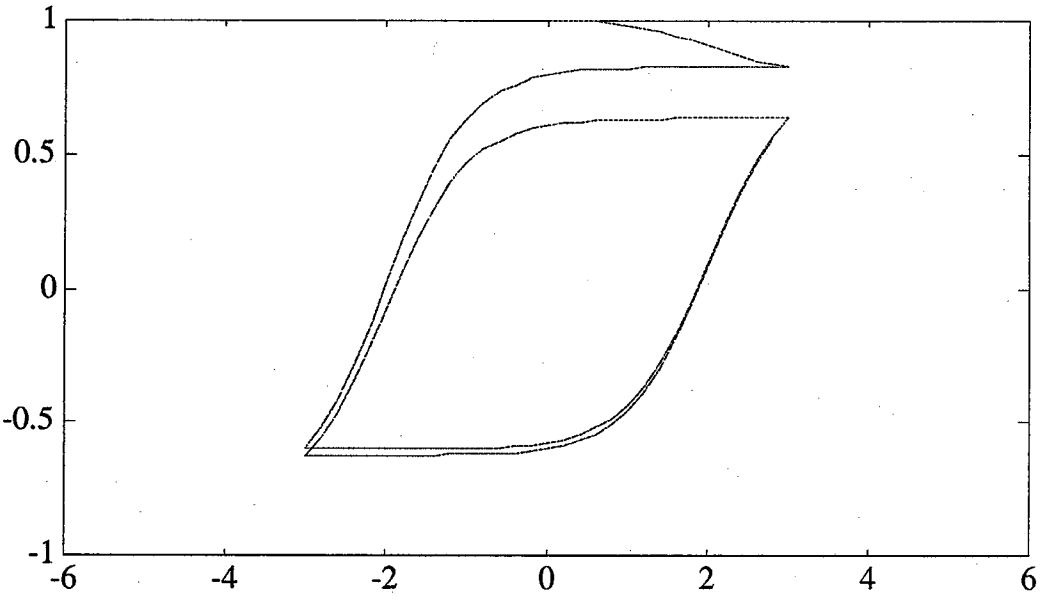

Figure 12. Convergence of the hystery unit when driven from (0,1).
The amplitude of the a.c. input is 3; Bs = 0.8; Hc = 2.

$$T_3 = \tanh(b + a + H_c);\ S_3 = \sinh(b + a + H_c);\ C_3 = \cosh(b + a + H_c)$$

$$T_4 = \tanh(b + a - H_c);\ S_4 = \sinh(b + a - H_c);\ C_4 = \cosh(b + a - H_c)$$

Combining Equations 58 and 59,

$$\eta^+_{k+1} = \frac{1}{1 - T_1}\left\{-T_1 + T_2 - \frac{1 + T_2}{1 + T_3}\left[T_3 - T_4 - (1 - T_4)\eta^+_k\right]\right\}$$

$$= \frac{T_2 - T_1}{1 - T_1} - \frac{1 + T_2}{1 + T_3}\frac{T_3 - T_4}{1 - T_1} + \frac{1 + T_2}{1 + T_3}\frac{1 - T_4}{1 - T_1}\eta^+_k \qquad (60)$$

Assuming there exists η^+ such that

$$\lim_{k\to\infty} \eta^+_{k+1} = \lim_{k\to\infty} \eta^+_k = \eta^+$$

Then, by taking the limit on both sides of Equation 60,

$$\eta^+ = \frac{T_2 - T_1}{1 - T_1} - \frac{1 + T_2}{1 + T_3}\frac{T_3 - T_4}{1 - T_1} + \frac{1 + T_2}{1 + T_3}\frac{1 - T_4}{1 - T_1}\eta^+ \qquad (61)$$

$$\eta^+ = \frac{(1 + T_3)(T_2 - T_1) - (1 + T_2)(T_3 - T_4)}{(1 + T_3)(1 - T_1) - (1 + T_2)(1 - T_4)} \qquad (62)$$

$$= \frac{(1 + \frac{S_3}{C_3})(\frac{S_2}{C_2} - \frac{S_1}{C_1}) - (1 + \frac{S_2}{C_2})(\frac{S_3}{C_3} - \frac{S_4}{C_4})}{(1 + \frac{S_3}{C_3})(1 - \frac{S_1}{C_1}) - (1 + \frac{S_2}{C_2})(1 - \frac{S_4}{C_4})}$$

$$= \frac{C_4(C_3 + S_3)(C_1S_2 - S_1C_2) - C_1(C_2 + S_2)(C_4S_3 - S_4C_3)}{C_2C_4(C_3 + S_3)(C_1 - S_1) - C_1C_3(C_2 + S_2)(C_4 - S_4)}$$

The following identities will be useful:

$$\cosh x + \sinh x = e^x$$

$$\cosh x - \sinh x = e^{-x}$$

$$\cosh x \cosh y = \frac{1}{2}[\cosh(x + y) + \cosh(x - y)]$$

$$\cosh x \sinh y - \sinh x \cosh y = \sinh(y - x)$$

Continuing, the numerator for η^+ is:

$$
\begin{aligned}
&C_4(C_3 + S_3)(C_1S_2 - S_1C_2) - C_1(C_2 + S_2)(C_4S_3 - S_4C_3) \\
&= \cosh\,(b + a - H_c)\, e^{b+a+H_c} \sinh 2H_c - \\
&\quad \cosh\,(b - a - H_c)\, e^{b-a+H_c} \sinh 2H_c \\
&= \sinh 2H_c \left[\cosh\,(b + a - H_c)\, e^{b+a+H_c} - \right. \\
&\qquad\qquad \left. \cosh\,(b - a - H_c)\, e^{b-a+H_c}\right] \\
&= \frac{1}{2} \sinh 2H_c \,[e^{2(b+a)} + e^{2H_c} - e^{2(b-a)} - e^{2H_c}] \\
&= \frac{1}{2} \sinh 2H_c \,[e^{2(b+a)} - e^{2(b-a)}] \\
&= \frac{1}{2} \sinh 2H_c \,[e^{2a} - e^{-2a}]e^{2b}
\end{aligned}
\tag{63}
$$

The denominator in the expression for η^+ is:

$$
\begin{aligned}
&C_2C_4(C_3 + S_3)(C_1 - S_1) - C_1C_3(C_2 + S_2)(C_4 - S_4) \\
&= \frac{1}{2}[\cosh 2b + \cosh 2(a - H_c)]e^{b+a+H_c}e^{-b+a+H_c} - \\
&\quad \frac{1}{2}[\cosh 2b + \cosh 2(a + H_c)]e^{b-a+H_c}e^{-b-a+H_c} \\
&= \frac{1}{2} \cosh 2b \,[e^{2(a+H_c)} - e^{2(-a+H_c)}] + \\
&\quad \frac{1}{2}[\cosh 2(a - H_c)\, e^{2(a+H_c)} - \cosh 2(a + H_c)\, e^{2(-a+H_c)}] \\
&= \cosh 2b \sinh 2a\, e^{2H_c} + \frac{1}{4}[e^{4H_c} + e^{4a} - e^{-4a} - e^{4H_c}] \\
&= \cosh 2b \sinh 2a\, e^{2H_c} + \frac{1}{4}[e^{4a} - e^{-4a}]
\end{aligned}
\tag{64}
$$

Combining the numerator and denominator for η^+,

$$
\eta^+ = \frac{\frac{1}{2} \sinh 2H_c \,[e^{2a} - e^{-2a}]e^{2b}}{\cosh 2b \sinh 2a\, e^{2H_c} + \frac{1}{4}(e^{2a} + e^{-2a})(e^{2a} - e^{-2a})}
$$

$$= \frac{\sinh 2H_c \sinh 2a\, e^{2b}}{\cosh 2b \sinh 2a\, e^{2H_c} + \cosh 2a \sinh 2a}$$

$$= \frac{\sinh 2H_c\, e^{2b}}{\cosh 2a + \cosh 2b\, e^{2H_c}} \tag{65}$$

Note that if $b = 0$, then $\eta^+ = \eta = (\sinh 2H_c)/[\cosh 2a + \exp(2H_c)]$.

Next, it is shown below that if $\eta_k^+ > \eta^+$, then $\eta_{k+1}^+ > \eta^+$ also holds. Taking Equation 60, and let $\eta_k^+ > \eta^+$,

$$\eta_{k+1}^+ = \frac{T_2 - T_1}{1 - T_1} - \frac{1 + T_2}{1 + T_3}\frac{T_3 - T_4}{1 - T_1} + \frac{1 + T_2}{1 + T_3}\frac{1 - T_4}{1 - T_1}\eta_k^+$$

$$> \frac{T_2 - T_1}{1 - T_1} - \frac{1 + T_2}{1 + T_3}\frac{T_3 - T_4}{1 - T_1} + \frac{1 + T_2}{1 + T_3}\frac{1 - T_4}{1 - T_1}\eta^+ \tag{66}$$

$$(1 + T_3)(1 - T_1)\eta_{k+1}^+ > (1 + T_3)(T_2 - T_1) - (1 + T_2)(T_3 - T_4) + (1 + T_2)(1 - T_4)\eta^+ \tag{67}$$

Substituting in η^+ from Equation 62 in the right side of the inequality, it becomes:

$$(1 + T_3)(T_2 - T_1) - (1 + T_2)(T_3 - T_4) + (1 + T_2)(1 - T_4)\frac{(1 + T_3)(T_2 - T_1) - (1 + T_2)(T_3 - T_4)}{(1 + T_3)(1 - T_1) - (1 + T_2)(1 - T_4)}$$

$$= (1 + T_3)(T_2 - T_1) - (1 + T_2)(T_3 - T_4) + \frac{(1 + T_2)(1 - T_4)(1 + T_3)(T_2 - T_1) - (1 + T_2)(1 - T_4)(1 + T_2)(T_3 - T_4)}{(1 + T_3)(1 - T_1) - (1 + T_2)(1 - T_4)}$$

$$= \Big\{(1 + T_2)(1 - T_4)(1 + T_3)(T_2 - T_1) - (1 + T_2)(1 - T_4)(1 + T_2)(T_3 - T_4) + (1 + T_3)(T_2 - T_1)(1 + T_3)(1 - T_1) - (1 + T_3)(T_2 - T_1)(1 + T_2)(1 - T_4) - (1 + T_2)(T_3 - T_4)(1 + T_3)(1 - T_1) + (1 + T_2)(T_3 - T_4)(1 + T_2)(1 - T_4)\Big\} / \Big[(1 + T_3)(1 - T_1) - (1 + T_2)(1 - T_4)\Big]$$

$$= (1 + T_3)(1 - T_1)\frac{(1 + T_3)(T_2 - T_1) - (1 + T_2)(T_3 - T_4)}{(1 + T_3)(1 - T_1) - (1 + T_2)(1 - T_4)}$$

$$= (1 + T_3)(1 - T_1)\eta^+ \tag{68}$$

Therefore $(1 + T_3)(1 - T_1)\eta^+_{k+1} > (1 + T_3)(1 - T_1)\eta^+$, or $\eta^+_{k+1} > \eta^+$ follows from $\eta^+_k > \eta^+$. On the contrary, $\eta^+_{k+1} < \eta^+$ if $\eta^+_k < \eta^+$ holds.

The derivations below show that if $\eta^+_k > \eta^+$, then $\eta^+_{k+1} < \eta^+_k$ and the sequence $\{\eta^+_k\}$ is monotonically decreasing. Conversely, if $\eta^+_k < \eta^+$, then the sequence $\{\eta^+_k\}$ is monotonically increasing.

$$\eta^+_{k+1} - \eta^+_k = \frac{T_2 - T_1}{1 - T_1} - \frac{1 + T_2}{1 + T_3}\frac{T_3 - T_4}{1 - T_1} + \left(\frac{1 + T_2}{1 + T_3}\frac{1 - T_4}{1 - T_1} - 1\right)\eta^+_k \tag{69}$$

$$= \Big\{(1 + T_3)(T_2 - T_1) - (1 + T_2)(T_3 - T_4) + [(1 + T_2)(1 - T_4) - (1 + T_3)(1 - T_1)]\eta^+_k\Big\} \Big/ \Big[(1 + T_3)(1 - T_1)\Big]$$

Suppose $\eta^+_k > \eta^+$, then the numerator

$$\begin{aligned}
&(1 + T_3)(T_2 - T_1) - (1 + T_2)(T_3 - T_4) - \\
&\qquad [(1 + T_3)(1 - T_1) - (1 + T_2)(1 - T_4)]\eta^+_k \\
&< (1 + T_3)(T_2 - T_1) - (1 + T_2)(T_3 - T_4) - \\
&\qquad [(1 + T_3)(1 - T_1) - (1 + T_2)(1 - T_4)]\eta^+ \\
&= (1 + T_3)(T_2 - T_1) - (1 + T_2)(T_3 - T_4) - \\
&\quad [(1 + T_3)(T_2 - T_1) - (1 + T_2)(T_3 - T_4)] \\
&= 0
\end{aligned} \tag{70}$$

Thus, if $\eta^+_k > \eta^+$, then $\eta^+_{k+1} < \eta^+_k$, and the sequence $\{\eta^+_k\}$ is monotonically decreasing, converging to η^+. (Figure 13, odd time indices, upper half of the graph.) Conversely, if $\eta^+_k < \eta^+$, then $\eta^+_{k+1} > \eta^+_k$, and the sequence $\{\eta^+_k\}$ is monotonically increasing, converging to η^+. (Figure 14, odd time indices, upper half of the graph.)

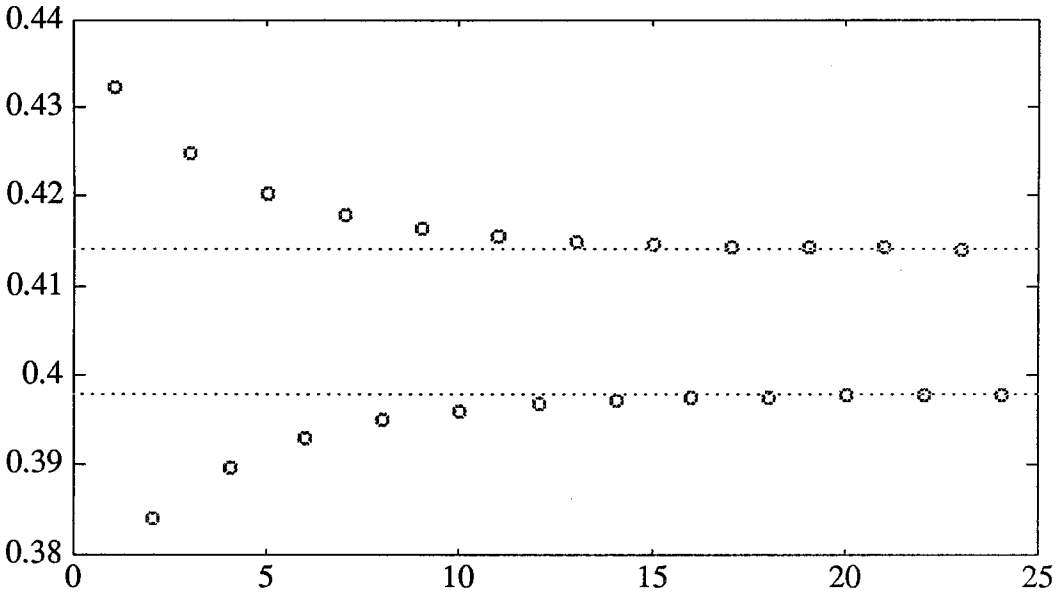

Figure 13. Convergence of the index into the family of curves under a bias of 0.01. The a.c. magnitude is 0.5; Bs = 1; Hc = 1; starting from (0,0).

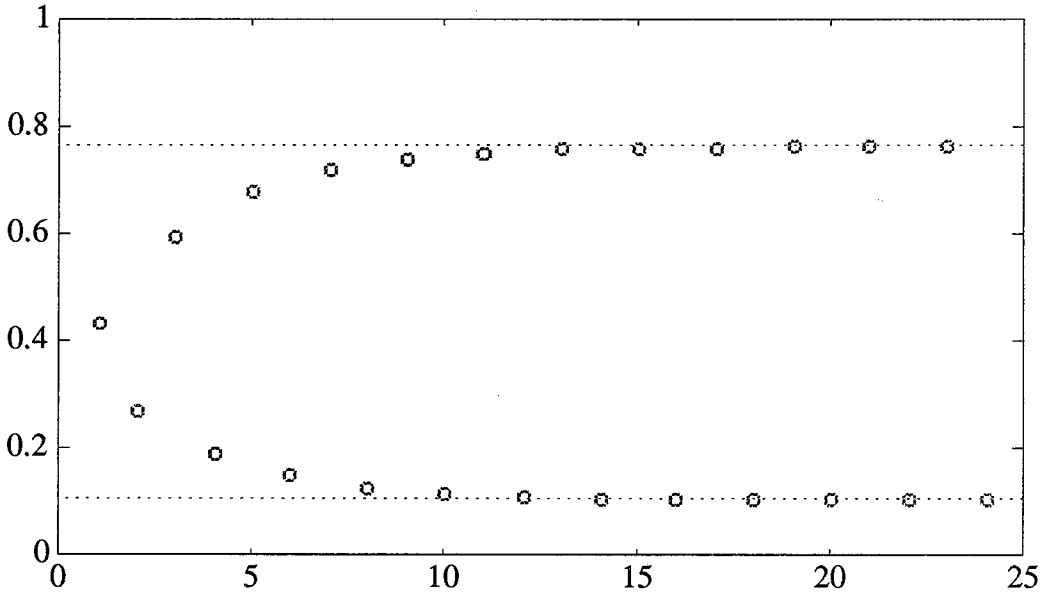

Figure 14. Convergence of the index into the family of curves under a bias of 0.5. The a.c. magnitude is 0.5; Bs = 1; Hc = 1; starting from (0,0).

To complete the second half of the proof of Theorem 1, here is the counterpart of Equation 60:

$$\eta_{k+1}^{-} = \frac{1}{1+T_3}\left\{T_3 - T_4 - \frac{1-T_4}{1-T_1}\left[-T_1 + T_2 - (1+T_2)\eta_k^{-}\right]\right\}$$

$$= \frac{T_3 - T_4}{1+T_3} - \frac{1-T_4}{1-T_1}\frac{T_2 - T_1}{1+T_3} + \frac{1-T_4}{1-T_1}\frac{1+T_2}{1+T_3}\eta_k^{-} \qquad (71)$$

Let $\lim_{k\to\infty} \eta_{k+1}^{-} = \lim_{k\to\infty} \eta_k^{-} = \eta^{-}$. Then,

$$\eta^{-} = \frac{(1-T_1)(T_3 - T_4) - (1-T_4)(T_2 - T_1)}{(1-T_1)(1+T_3) - (1-T_4)(1+T_2)} \qquad (72)$$

By going through a similar derivation, or by observing -b may be substituted for b in the solution for η^{+},

$$\eta^{-} = \frac{\sinh 2H_c\, e^{-2b}}{\cosh 2a + \cosh 2b\, e^{2H_c}} \qquad (73)$$

If $\eta_k^{-} < \eta^{-}$, then

$$\eta_{k+1}^{-} < \frac{T_3 - T_4}{1+T_3} - \frac{1-T_4}{1-T_1}\frac{T_2 - T_1}{1+T_3} + \frac{1-T_4}{1-T_1}\frac{1+T_3}{1+T_3}\eta^{-} \qquad (74)$$

Following the derivations above in a similar fashion,

$$\eta_{k+1}^{-} < \eta^{-} \qquad (75)$$

Or if $\eta_k^{-} > \eta^{-}$, then $\eta_{k+1}^{-} > \eta^{-}$. The difference of η_{k+1}^{-} and η_k^{-} is:

$$\eta_{k+1}^{-} - \eta_k^{-} = \frac{T_3 - T_4}{1+T_3} - \frac{1-T_4}{1-T_1}\frac{T_2 - T_1}{1+T_3} + \left[\frac{1-T_4}{1-T_1}\frac{1+T_3}{1+T_3} - 1\right]\eta_k^{-}$$

Again, following the above derivations, $\eta_{k+1}^{-} > \eta_k^{-}$ if $\eta_k^{-} < \eta^{-}$, and the sequence $\{\eta_k^{-}\}$ is monotonically increasing, converging to η^{-}. (Figure 13, even time indices, lower half of the graph.) Conversely, if $\eta_k^{-} > \eta^{-}$, then $\eta_{k+1}^{-} < \eta_k^{-}$, and the sequence $\{\eta_k^{-}\}$ is monotonically decreasing, converging to η^{-}. (Figure 14, even time indices, lower half of the graph.) This completes the proof of Theorem 1. Similar to Theorem 2, the proof of Theorem 1 is independent of a,

the magnitude of the a.c. input, and b, the d.c. bias. Figure 15 shows some loops with constant bias and various magnitudes. Figure 16 is generated with a bias larger than that in Figure 15. Figure 17 is generated with a fixed magnitude a.c. while the bias is varied.

Some Interesting Observations

From the proof above of Theorem 1, it can be seen that if $\eta_1^+ > \eta^+$, then $\{\eta_k^+\}$ converges to η^+ from above. If $\eta_1^+ < \eta^+$, then $\{\eta_k^+\}$ converges to η^+ from below. Now the interesting situation is that if $\eta_1^+ = \eta^+$, then $\eta_k^+ = \eta^+$ for all k, and convergence is immediate. Suppose the a.c. is applied while the system is at rest, that is, $(x_0, y_0) = (0, 0)$. It would be interesting to find a value for the magnitude a, given some b and H_c, for which convergence is immediate. Or for some a and H_c, a value for b can be found such that convergence is immediate. Without loss of generality, assume $x_1^+ = b + a$. Then

$$\begin{aligned}
\eta_1^+ &= \frac{0 - \tanh(-H_c)}{1 - \tanh(-H_c)} \\
&= \frac{\tanh H_c}{1 + \tanh H_c} \\
&= \frac{e^{H_c} - e^{-H_c}}{e^{H_c} + e^{-H_c} + e^{H_c} - e^{-H_c}} \\
&= \frac{e^{H_c} - e^{-H_c}}{2e^{H_c}} \\
&= \frac{1}{2}(1 - e^{-2H_c}) \qquad (76)
\end{aligned}$$

$$\eta^+ = \frac{\sinh 2H_c\, e^{2b}}{\cosh 2a + \cosh 2b\, e^{2H_c}} \qquad (77)$$

Equating η_1^+ and η^+ and solving for a,

$$\frac{1}{2}(1 - e^{-2H_c}) = \frac{\sinh 2H_c\, e^{2b}}{\cosh 2a + \cosh 2b\, e^{2H_c}}$$

$$\cosh 2a = \frac{2 \sinh 2H_c\, e^{2b}}{1 - e^{-2H_c}} - \cosh 2b\, e^{2H_c}$$

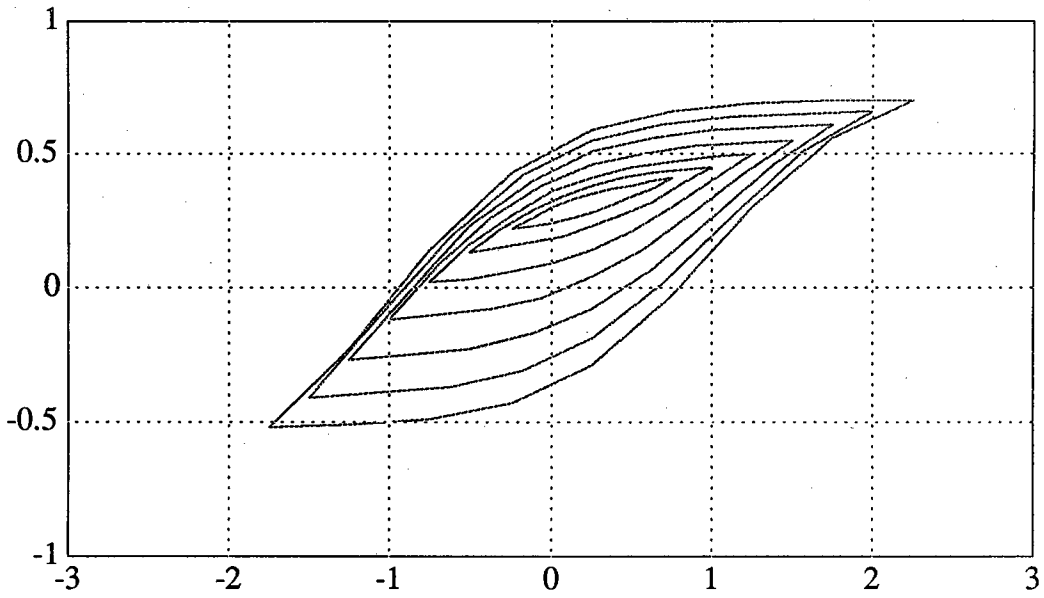

Figure 15. Several steady state loops of the hystery unit when driven by biased a.c. The bias is 0.25; Bs = 0.8; Hc = 1. The inner through the outer loops are driven by a.c. of magnitudes 0.5, 0.75, 1, 1.25, 1.5, 1.75, and 2 respectively.

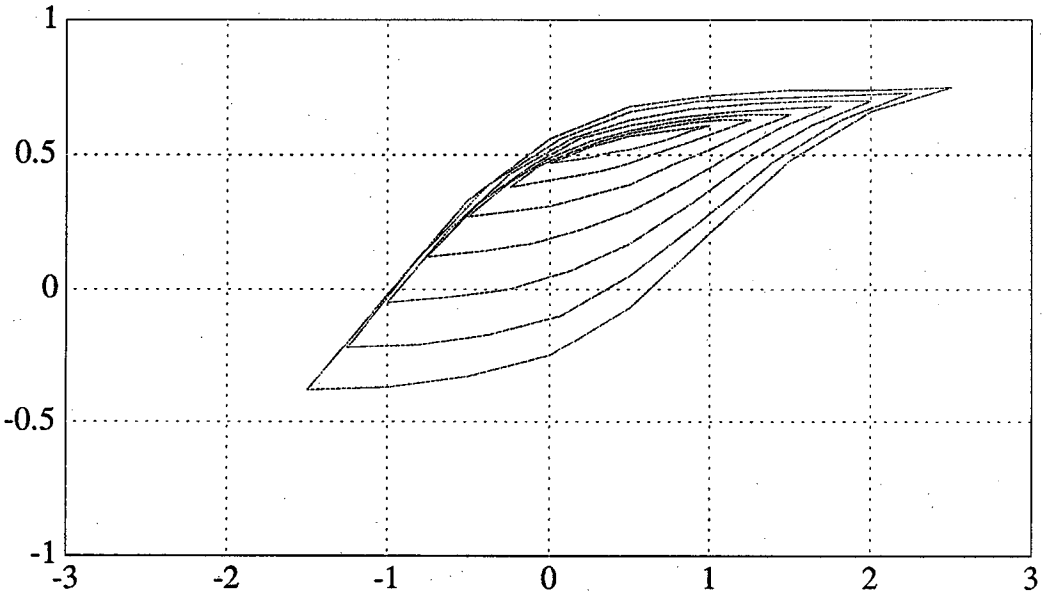

Figure 16. Several steady state loops of the hystery unit when driven by biased a.c. The bias is 0.5; Bs = 0.8; Hc = 1. The inner through the outer loops are driven by a.c. of magnitudes 0.5, 0.75, 1, 1.25, 1.5, 1.75, and 2 respectively.

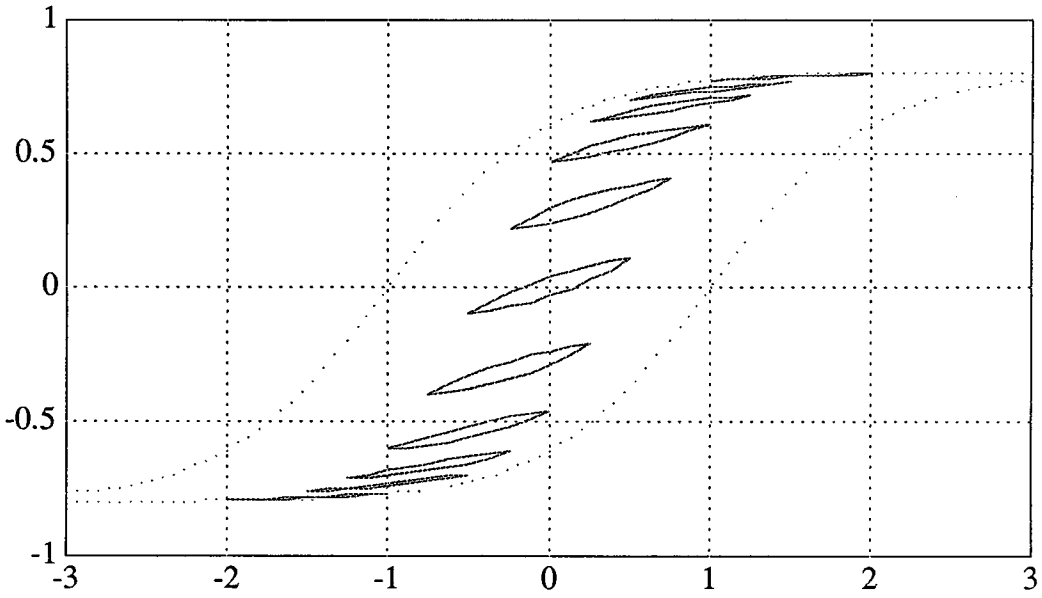

Figure 17. Several steady state loops of the hystery unit when driven by biased a.c. The magnitude is 0.5; Bs = 0.8; Hc = 1. The bottom through the top loops are driven by a.c. of bias -1.5, -1, -0.75, -0.5, -0.25, 0, 0.25, 0.5, 0.75, 1, and 1.5 respectively.

$$a = \frac{1}{2} \cosh^{-1}\left(\frac{2 \sinh 2H_c\, e^{2b}}{1 - e^{-2H_c}} - \cosh 2b\, e^{2H_c}\right) \tag{78}$$

If we solve for b instead,

$$\frac{2 \sinh 2H_c\, e^{2b}}{1 - e^{-2H_c}} = \cosh 2a + \cosh 2b\, e^{2H_c}$$

$$\frac{2 \sinh 2H_c\, e^{2b}}{1 - e^{-2H_c}} = \cosh 2a + (e^{2b} + e^{-2b})\, \frac{e^{2H_c}}{2}$$

$$e^{2b}\left[\frac{e^{2H_c}}{2} - \frac{2 \sinh 2H_c}{1 - e^{-2H_c}}\right] + \cosh 2a + e^{-2b}\left[\frac{e^{2H_c}}{2}\right] = 0 \tag{79}$$

The above equation is a quadratic in e^{2b}, and therefore b can be easily solved. Similarly if we arrange in terms of e^{2H_c},

$$\frac{1}{2}(1 - e^{-2H_c}) = \frac{\sinh 2H_c\, e^{2b}}{\cosh 2a + \cosh 2b\, e^{2H_c}}$$

$$2 \sinh (2H_c)\, e^{2b} = (1 - e^{-2H_c})[\cosh 2a + \cosh 2b\, e^{2H_c}]$$

$$(e^{2H_c} - e^{-2H_c})e^{2b} = \cosh 2a - \cosh 2a\, e^{-2H_c} + \cosh 2b\, e^{2H_c} - \cosh 2b$$

$$e^{2H_c}(e^{2b} - \cosh 2b) + (\cosh 2b - \cosh 2a) + e^{-2H_c}(\cosh 2a - e^{2b}) = 0 \tag{80}$$

H_c can be easily obtained as the above is a quadratic in e^{2H_c}.

One more interesting point to note is that the hystery unit is essentially the same as Model 1, the Differential Equation Model. With the hystery unit, there is no need to use numerical approximation to the solution of the differential equations of Model 1. Taking the derivative of a member of the rising curve, indexed by η, gives:

$$\frac{dy}{dx} = (1 - \eta)\, \frac{d}{dx} \tanh (x - H_c)$$

$$= (1 - \eta)[1 - \tanh^2 (x - H_c)]$$

$$= (1 - y_0)\frac{1 - \tanh^2 (x - H_c)}{1 - \tanh (x_0 - H_c)} \tag{81}$$

As this member passes through (x_0, y_0), the slope at this point is:

$$\left.\frac{dy}{dx}\right|_{(x_0,y_0)} = (1 - y_0)[1 + \tanh(x_0 - H_c)] \tag{82}$$

In general, the slope of the rising curves through (x, y) is $(1 - y)[1 + \tanh(x - H_c)]$. Deriving the slope of the falling curves in a similar manner gives $(1 + y)[1 + \tanh(-x - H_c)]$. Therefore, Model 4, the hystery unit, is identical to the Differential Equation Model. The difference is that the set of coupled differential equations are solved, and approximations to the solution is not required.

The Full Memory Conjecture

One of the motivations for modeling a neuron's adaptation behavior is to link this behavior with the memory or storage characteristics that is found in magnetic materials. With the models discussed above, their memory characteristics are studied with sequences of excitations. Here, the excitation is applied to the hystery unit starting from rest (zero initial output value). The excitation is bipolar, (analogous to the injection of a fixed amount of charge into the nerve cell) and is integrated for each time step (as in delta modulation). Figure 18 is a plot of the final coordinates of the inputs and the outputs of the hystery unit. Here the dashed lines show the members of the families of rising and falling curves with $\eta = 1$. Each dot is a final coordinate. The horizontal axis is the integral of a bipolar sequence (+ and −) of 7 steps. The vertical axis is the output of the hystery unit, with the parameters $B_s = 0.8$, $H_c = 1.0$, and a step size of 0.4. Since the integral of the bipolar sequence with a fixed step size can only have discrete values, thus the plot shows the final coordinates line up vertically at several discrete values on the horizontal axis. However, no two final coordinates overlap. Even when the step size is varied, as in Figures 19 and 20 (6 steps 0.4/0.5), the final coordinates remain separate. Moreover, Figure 21 shows that the intermediate coordinates are all different. More strikingly, when all these intermediate and final coordinates are projected onto the vertical axis, (that is, looking only at the output value alone) they remain distinct. Within the accuracy of the computation system, we have achieved the above result for

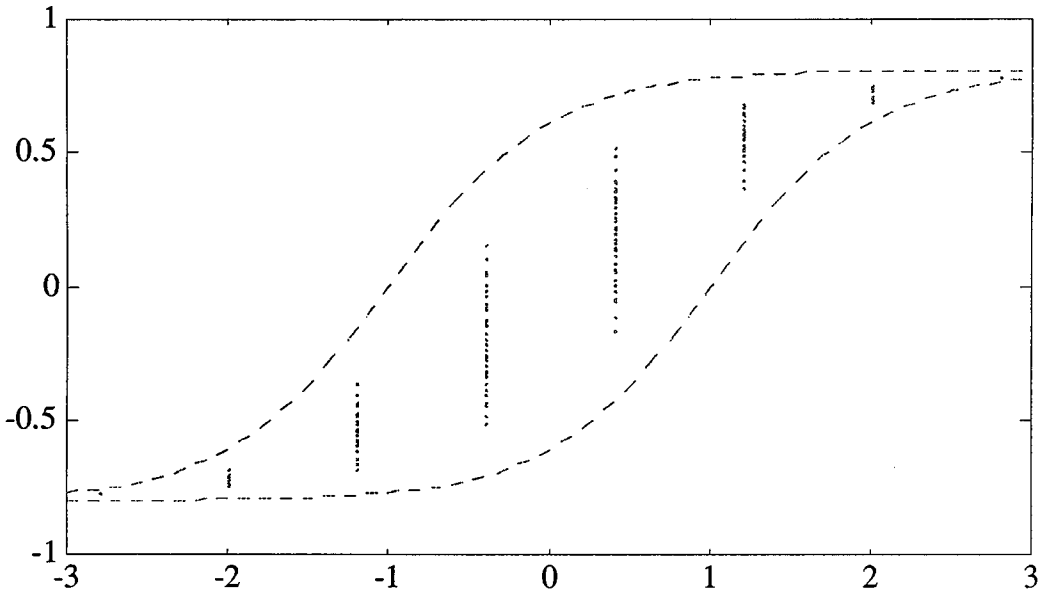

Figure 18. Final coordinates of all input sequences of 7 quantized steps. The step size is 0.4; Bs = 0.8; Hc = 1.

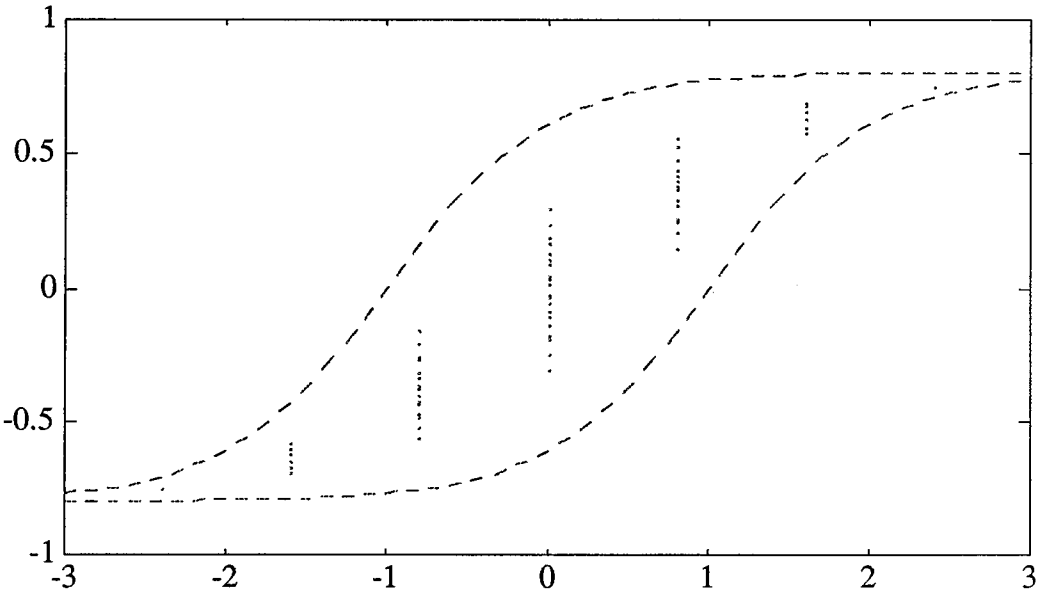

Figure 19. Final coordinates of all input sequences of 6 quantized steps. The step size is 0.4; Bs = 0.8; Hc = 1.

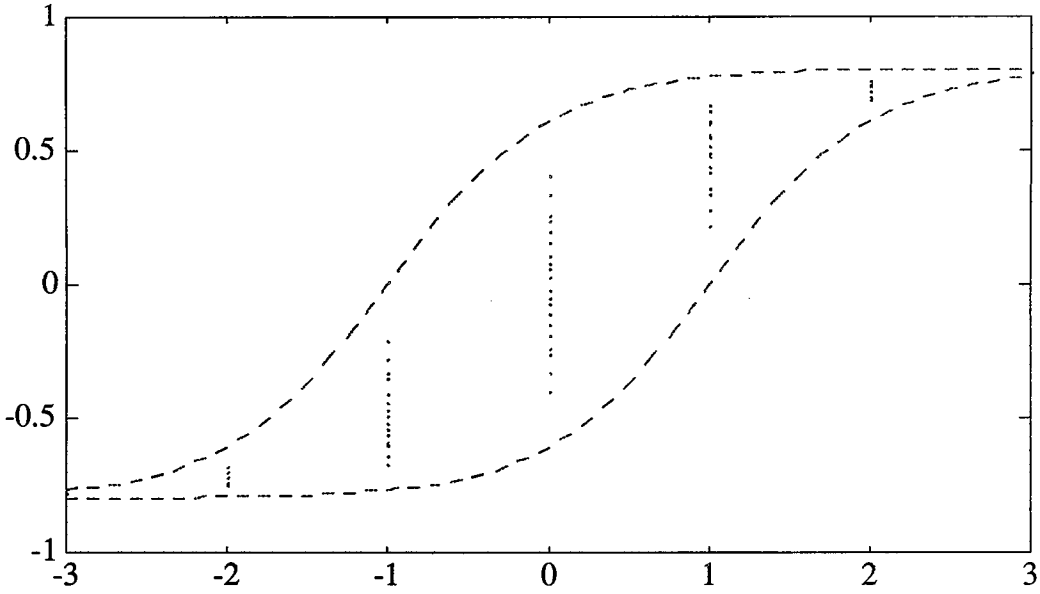

Figure 20. Final coordinates of all input sequences of 6 quantized steps. The step size is 0.5; Bs = 0.8; Hc = 1.

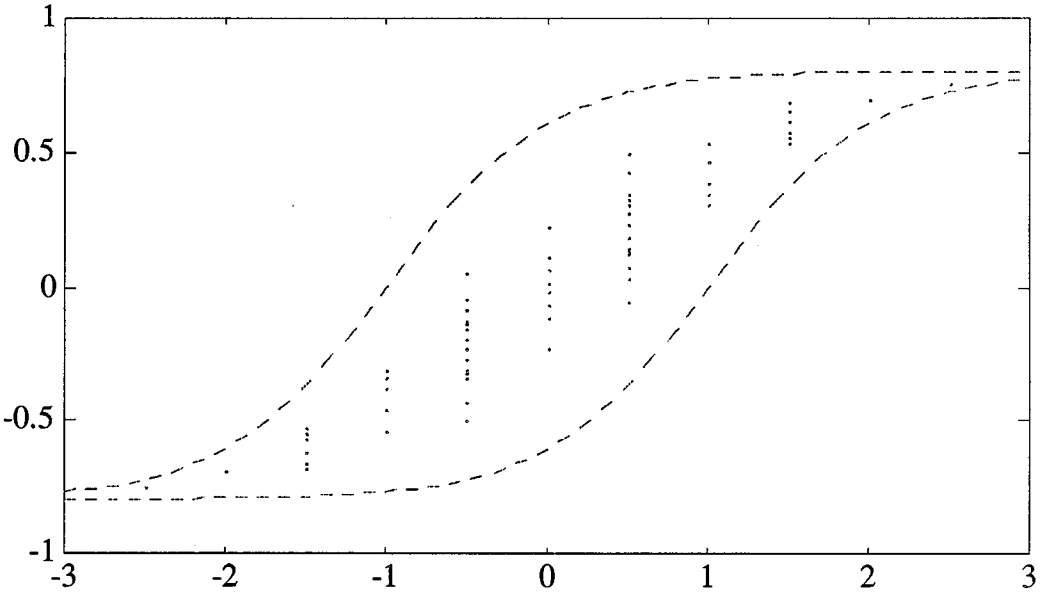

Figure 21. Final and intermediate coordinates of all input sequences of 5 quantized steps. The step size is 0.5; Bs = 0.8; Hc = 1.

all 1024 bipolar sequences of 10 steps, as well as all 1024 intermediary steps.

From the characteristics observed above, we conjecture the following:

> The final as well as the intermediary outputs of the hystery unit are all distinct. Thus when an output of the hystery unit is known, and given that it is initially at rest, there is a unique delta modulation input sequence that would drive the hystery unit to that particular output. The hystery unit thus retains the full history of its inputs.

Effect of Step Size

It is observed that with a large step size, most output values of the hystery unit are concentrated near $+B_s$ and $-B_s$. To observe the effect of step size, the output values within different ranges are tabulated, as shown in the histograms of Figures 22 through 25. Figures 22 and 24, and Figures 23 and 25 show that decreasing the step size results in the reduction of output values close to the extreme, and the concentration of output values near zero. Figure 25 shows that with bipolar sequences of 10 steps, the distribution is about even with a step size of 0.4, whereas for bipolar sequences of 7 steps in Figure 22, a step size of 0.5 gives similar result.

Sorting Behavior

From the outputs of the hystery unit in respond to various input sequences, it is observed that there is a relationship between the input sequence and the final output. For example, with an input sequence of 4 steps, "− − − −" always gives the smallest output while "+ + + +" always gives the largest output. Sequences with a single "+" (which have -2 as the accumulated input with three "−" and a "+") are sorted as "− − − +", "− − + −", "− + − −", and "+ − − −" from the smallest to the largest. Similarly, sequences with a single "−" (which have 2 as the accumulated input with three "+" and a "−") are sorted as "− + + +", "+ − + +", "+ + − +", and "+ + + −" from the smallest to the largest. The following argument shows that this can be the case for an input of any length.

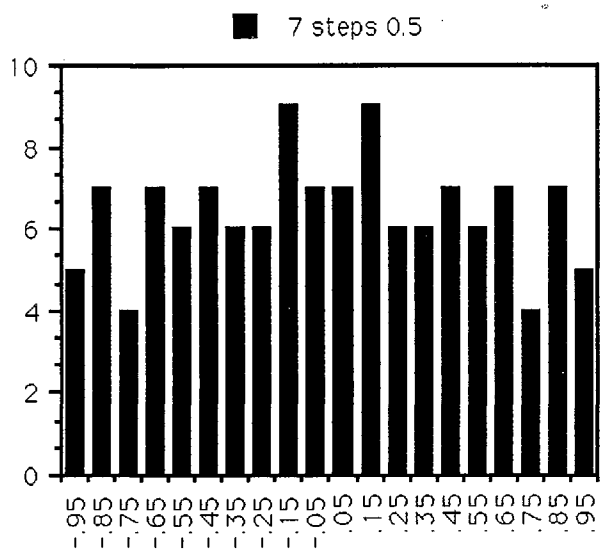

Figure 22. Density of the final output values for sequences of 7 quantized steps of step size 0.5.

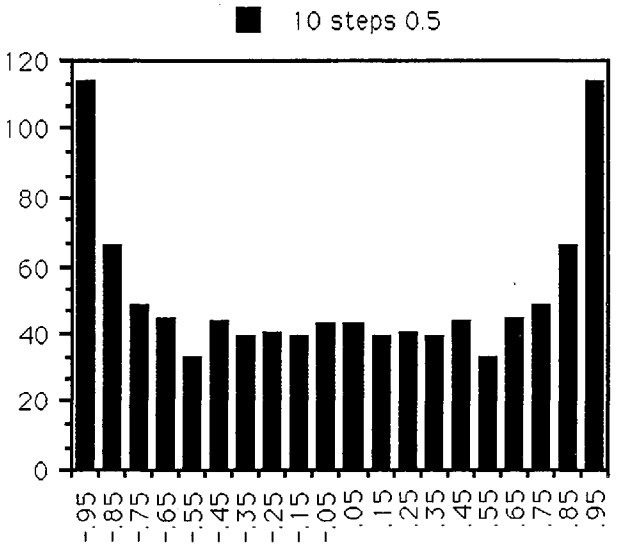

Figure 23. Density of the final output values for sequences of 10 quantized steps of step size 0.5.

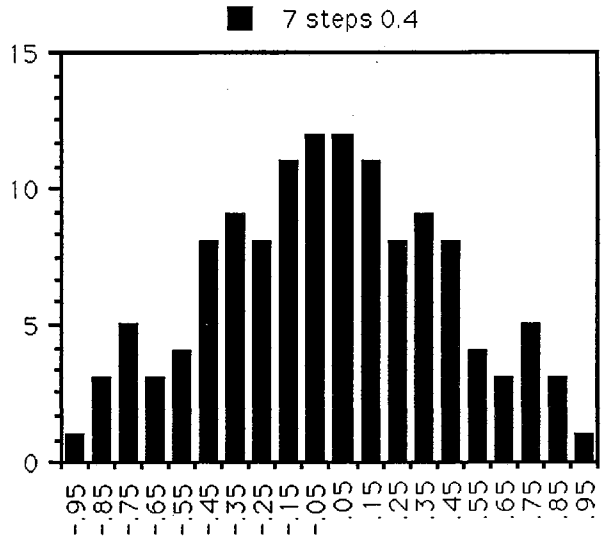

Figure 24. Density of the final output values for sequences of 7 quantized steps of step size 0.4.

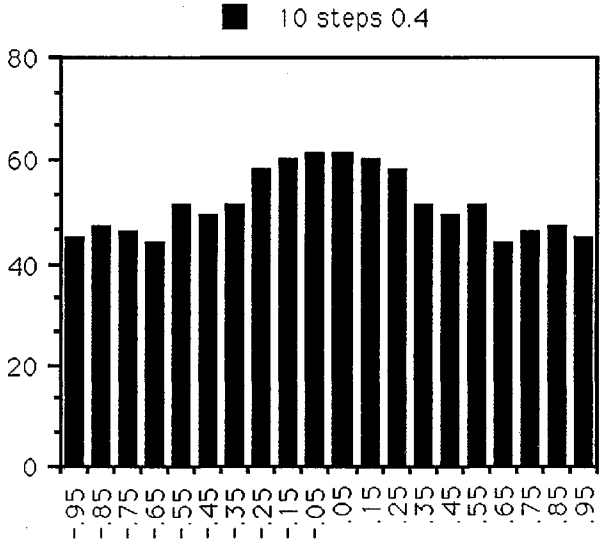

Figure 25. Density of the final output values for sequences of 10 quantized steps of step size 0.4.

Consider the four sequences above with a single "−". To show that the first sequence produces a smaller output than the second sequence does, we only have to consider the left-most sub-sequences of length 2, which are "− +" and "+ −". The rest of the two inputs are identical, and since the family of rising curves are non-intersecting, the result holds for the rest of the input sequences. To show that the second sequence produces a smaller output than the third, only the middle sub-sequences of length 2 need to be considered. They are also "− +" and "+ −". Using the above property of the family of rising curves, the result holds for the rest for the sequence. The result can be compounded with that for the first two sequences. In a similar manner, the fourth sequence can be iteratively included, producing the sorted output for the four input sequences.

Now let us consider the critical part, which is to show that the sequence "− +" always produces a smaller output than "+ −" when starting from the same point. Let the starting point be (x_k, y_k), and let the step size be a. Consider the first input sequence "− +". Then $x^-_{k+1} = x_k - a$, and $x^-_{k+2} = x_k$. Similarly, for the second input sequence "+ −", $x^+_{k+1} = x_k + a$, and $x^+_{k+2} = x_k$.

$$y^-_{k+1} = \tanh(x_k - a + H_c) - \left[1 + \tanh(x_k - a + H_c)\right] \frac{y_k - \tanh(x_k + H_c)}{-1 - \tanh(x_k + H_c)}$$

$$y^-_{k+2} = \tanh(x_k - H_c) + \left[1 + \tanh(x_k - H_c)\right] \frac{y^-_{k+1} - \tanh(x_k - a - H_c)}{1 - \tanh(x_k - a - H_c)}$$

$$y^+_{k+1} = \tanh(x_k + a - H_c) + \left[1 - \tanh(x_k + a - H_c)\right] \frac{y_k - \tanh(x_k - H_c)}{1 - \tanh(x_k - H_c)}$$

$$y^+_{k+2} = \tanh(x_k + H_c) - \left[1 + \tanh(x_k + H_c)\right] \frac{y^+_{k+1} - \tanh(x_k + a + H_c)}{-1 - \tanh(x_k + a + H_c)}$$

The 3-D plot of $z = y^+_{k+2} - y^-_{k+2}$ is shown in Figure 26, and is positive in the x,y-plane. Figure 27 shows that the cross section of the plot of z is above zero along the "magnetization curve" of the hystery unit. As defined earlier, the "magnetization curve" is not an exception as defined in Model 3, but is composed of a member of each of the families of rising and falling curves that pass through the origin.

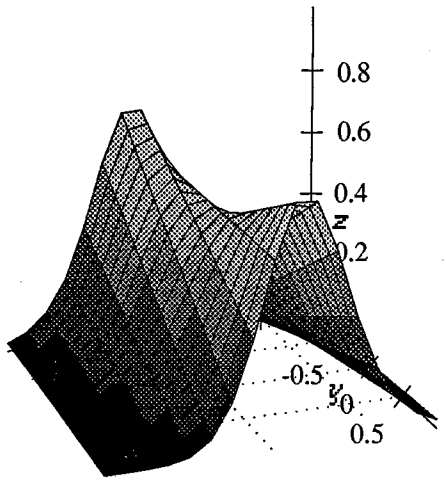

Figure 26. $z = y^{+}_{k+2} - y^{-}_{k+2}$ plotted over the x,y-plane with x ranging from -3 to 3 and y ranging from -1 to 1. Within this region, z is positive.

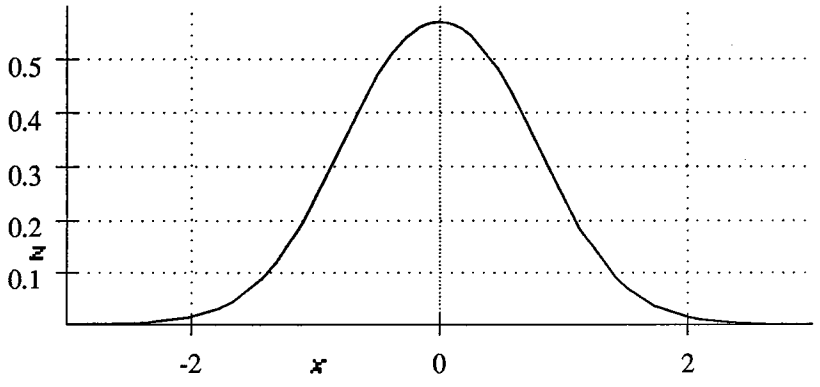

Figure 27. $z = y^{+}_{k+2} - y^{-}_{k+2}$ plotted along the curve through the origin (the "magnetization curve" of the hystery unit).

Application - Simple Spatiotemporal Pattern Recognition

In this section, the hystery unit is used as a nonlinear memory device in the classification of spatiotemporal patterns. A spatiotemporal pattern is a spatial pattern that is continuous, or at least piecewise continuous in time. To simplify the problem, time-varying spatial patterns in one dimension are classified with the aid of the hystery unit. The number of spatial dimensions is not at issue here, since the hystery unit operates on the time dimension of the output of another classifier - the MIND unit. ("MIND" is an acronym for multivariate independent normal distribution. The MIND unit gives an inverse distance measure of the input in relation to a class distribution.) The number of spatial dimensions affects only the architecture of the MIND unit.

The characteristic of the hystery unit that is employed here is specifically the nonlinearity of its memory. Inputs of two MIND units, one for class A, and the other for class B, are subtracted (just as neurons in motion analysis), the difference is accumulated (as ions accumulate inside the membrane of a neuron), and the accumulator's output feeds into the hystery unit. Essentially the accumulator adds up all the scores for class A, and subtracts from it all those for class B. The accumulator gives zero output when the total scores for class A equals the totals for class B. However, the hystery unit operates differently. Even when the accumulator reaches zero, the hystery unit output does not reach zero. There is a residue bias for one class over the other. Only when the accumulator bias for the other class is substantial would the hystery unit give zero output.

To test the behavior of the hystery unit, simple spatiotemporal patterns are created. These patterns vary in a one-dimensional space and in time. One set of patterns created is called the X-patterns. These patterns have two paths that cross. One path generally increases in time its spatial magnitude, while the other has decreasing magnitude in time.

Non-stationary noise is superimposed onto the X-patterns to create noisy patterns. A total of 9 noisy X-patterns are created for testing, as shown in Figure 28. The underlying noise process has a variance that is controlled so that it is large at the beginning, small in the middle, and grows again toward the

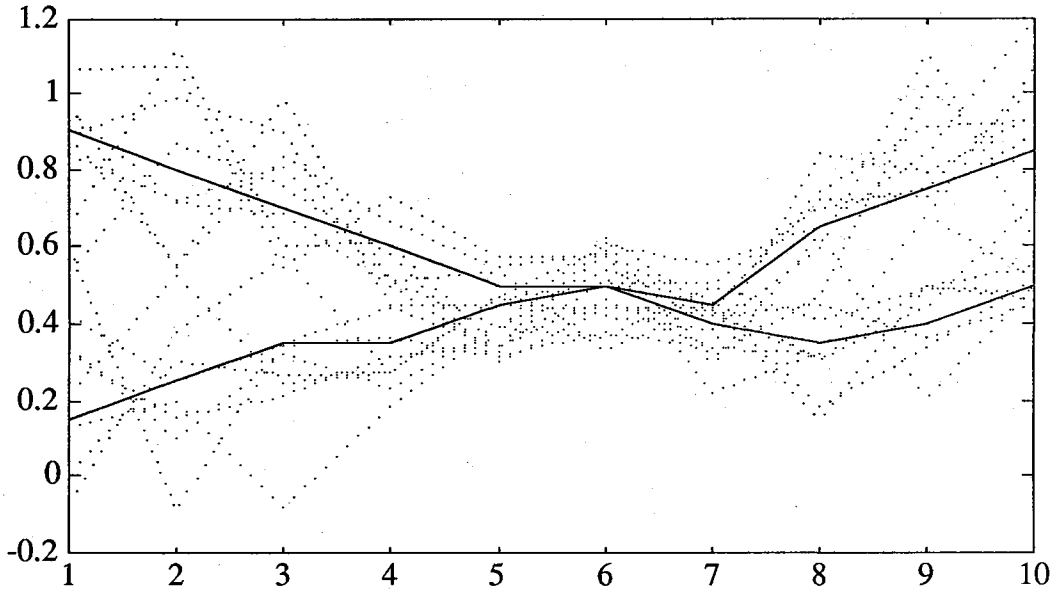

Figure 28. The X-patterns (solid line) and 9 noise corrupted X-patterns (dotted lines). The noise has a large variance in the beginning and at the end, but has a small variance in the middle.

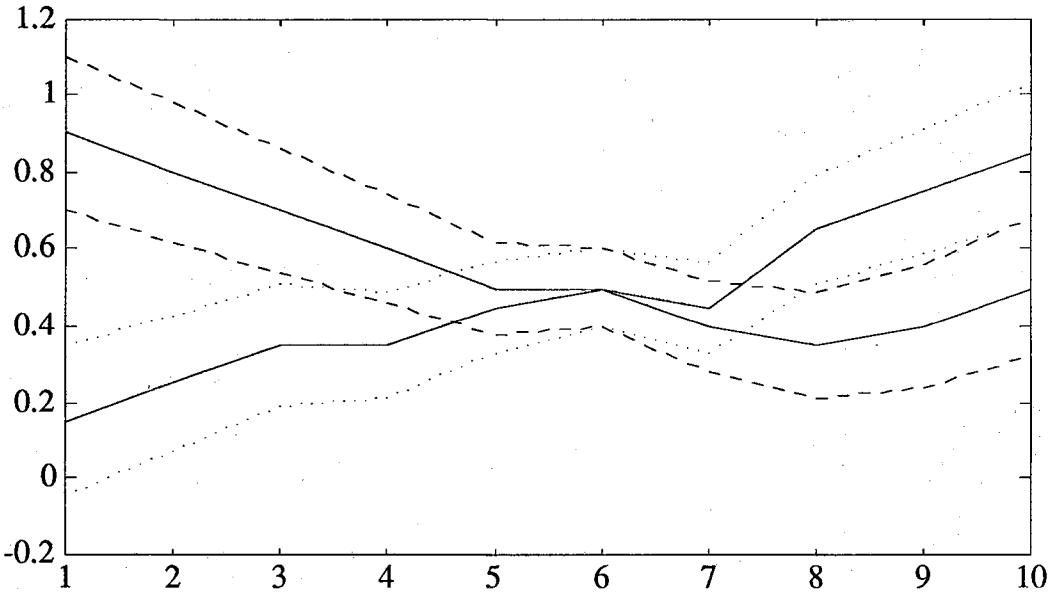

Figure 29. The X-patterns and the 1-standard deviation margin of the noise which has a large variance in the beginning and at the end, but small in the middle.

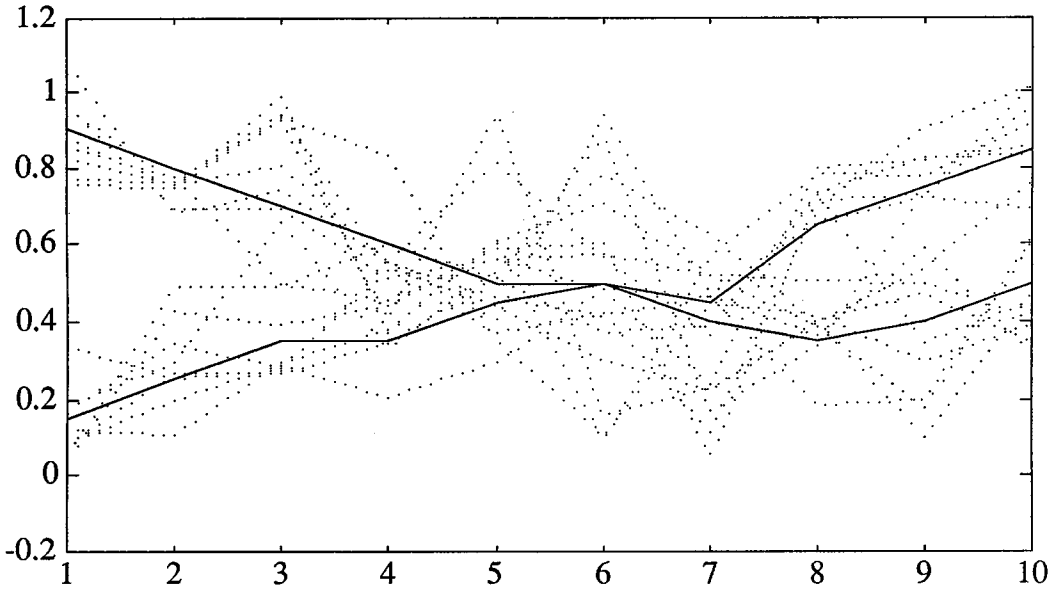

Figure 30. The X-patterns (solid line) and 9 noise corrupted X-patterns (dotted lines). The noise has a small variance in the beginning and at the end, but has a large variance in the middle. Note that the patterns are easily distinguishable just by looking at the beginning.

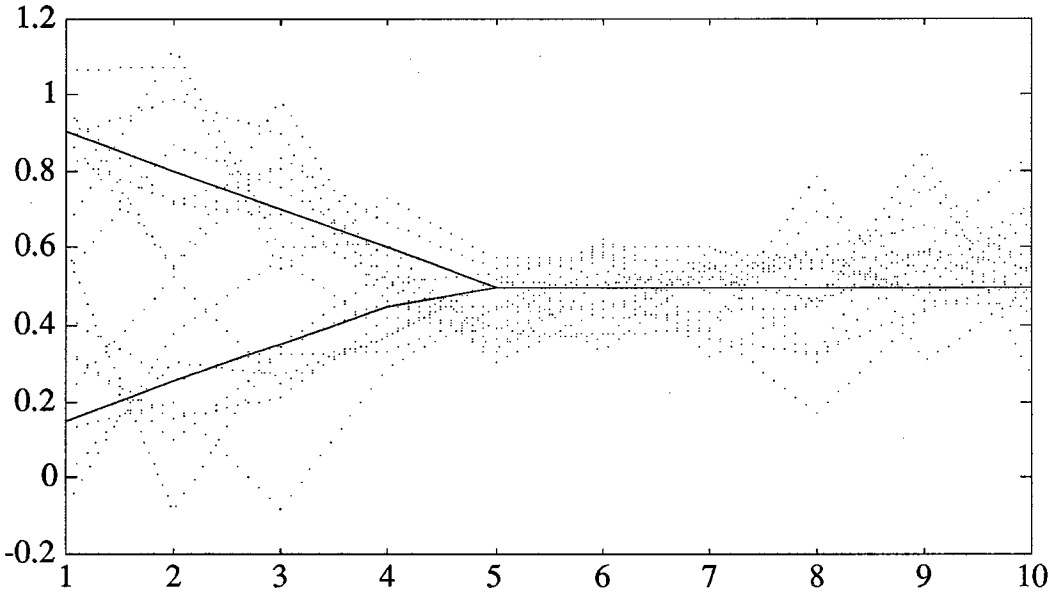

Figure 31. The Y-patterns (solid line) and 9 noise corrupted Y-patterns (dotted lines).

end. (Figure 29.) This noise process confuses the two paths more than a noise with constant variance, or a noise process with small variance at the beginning and the end, and a large variance in the middle. (Figure 30.) As seen from Figure 30, the paths are distinguishable simply by looking at the beginning of the pattern, where the X-patterns are maximally separable.

The other set of patterns generated are called the Y-patterns, They are similar to the X-patterns except that the two paths converge in the middle, and remain the same through the end. The reverse Y-patterns would be the above with the paths diverging. Again, non-stationary noise is added to the paths. The noise variance is large at the beginning and at the end, and small in the middle. (Figure 31.)

The results of the hystery unit classification for several of these noise patterns are shown in Figures 32-37. Figures 32 and 33 show the result of the classification of a noisy path generated with the one path of the Y-patterns with increasing magnitude. Figure 34 are those of the other path with decreasing magnitude. Figures 35-37 are the reversed Y-patterns of the three just mentioned above.

Figure 32 shows a very typical recognition result. At the beginning of the pattern, the difference between the two paths are large (dashed line), so that the cumulative score increases. This drives the hystery unit output high and keeps it there.

Figure 33 shows a not so typical noisy path, where at time step 3 the input is closer to the other path. Here the MIND unit gives a lower output, and thus the difference is negative. Note that the cumulative score decreases quite a bit while the hystery unit output stays almost the same. The same can be observed at time step 7.

Figure 34 shows the result with the Y-pattern path with decreasing magnitude. Observe that at time steps 5, 6, 7, 9, and 10, The MIND units classifies the noisy input to be closer to the other path. The hystery unit output stays almost the same. It is unaffected by a slight unfavorable evidence. Note that the cumulative score has dropped more than one-fourth of its peak value.

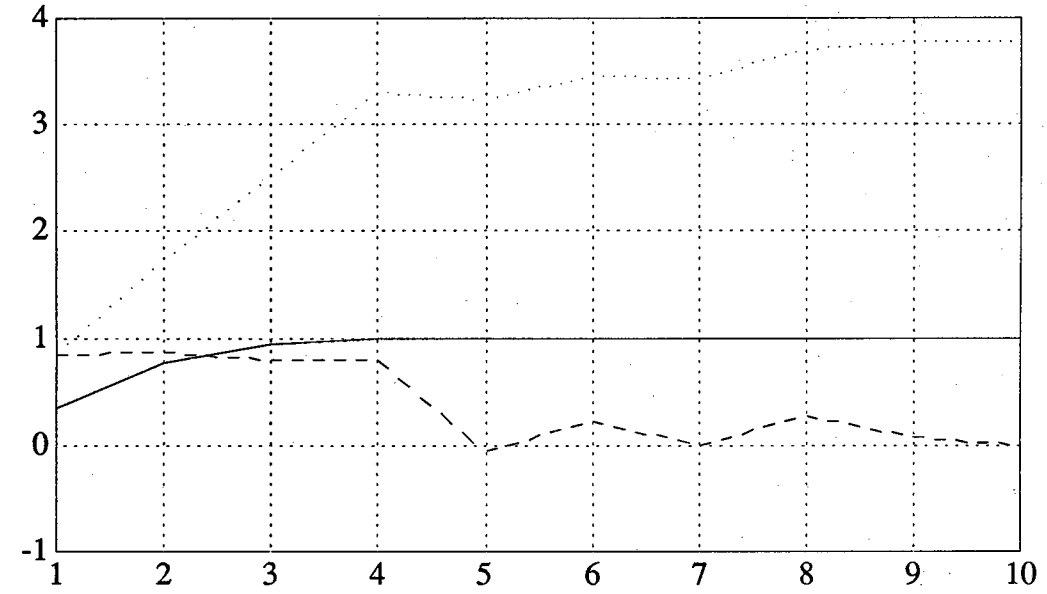

Figure 32. Recognition result with a noisy Y-pattern. The dashed line shows the difference between two MIND units trained on different paths. The dotted line shows the cumulative score of the difference. The solid line shows the output of the hystery unit.

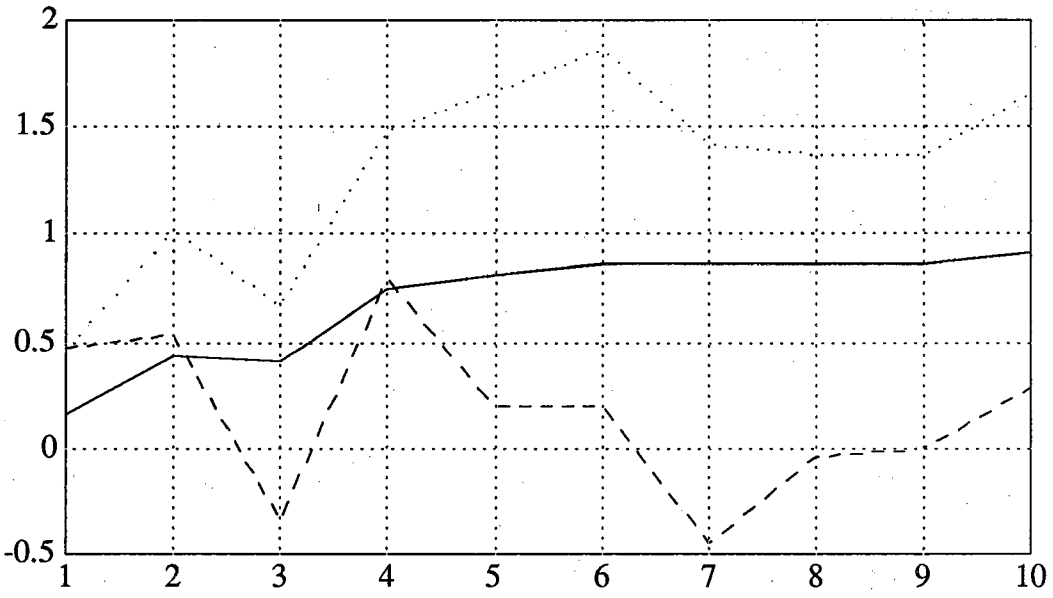

Figure 33. Recognition of a very noisy path of the Y-patterns. At time steps 3 and 7, the input sample is actually closer to the other path, causing the MIND unit to give a higher score for the other path. The cumulative difference decreases, yet the hystery unit's output is able to stay almost the same.

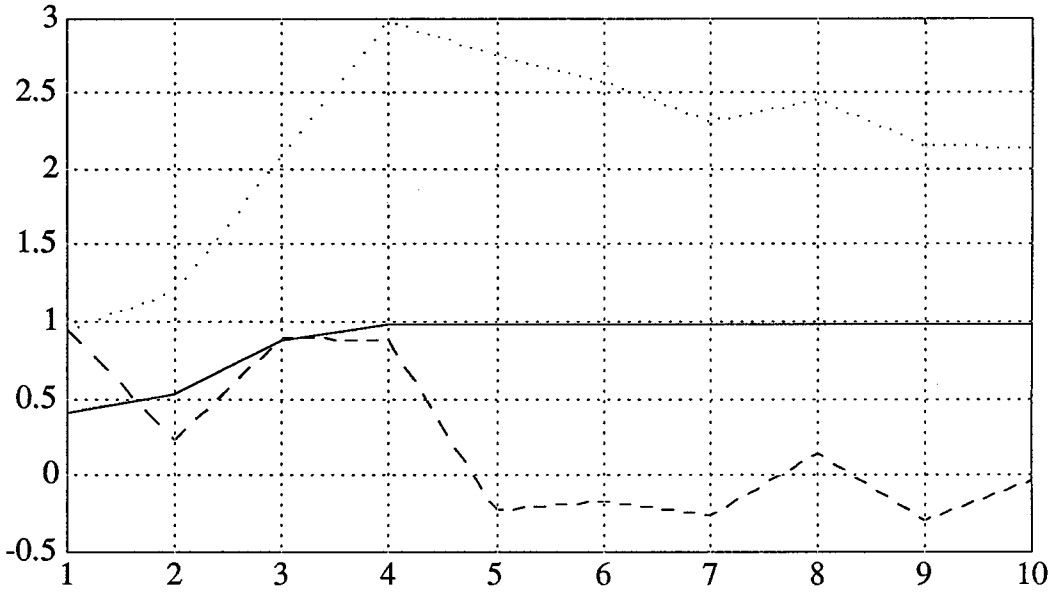

Figure 34. Recognition result of the other Y-pattern path that has decreasing magnitude. Note that at time steps 5, 6, 7, 9, and 10 the cumulative difference decreases to 3/4 of its peak value, yet the hystery unit holds on to its output value.

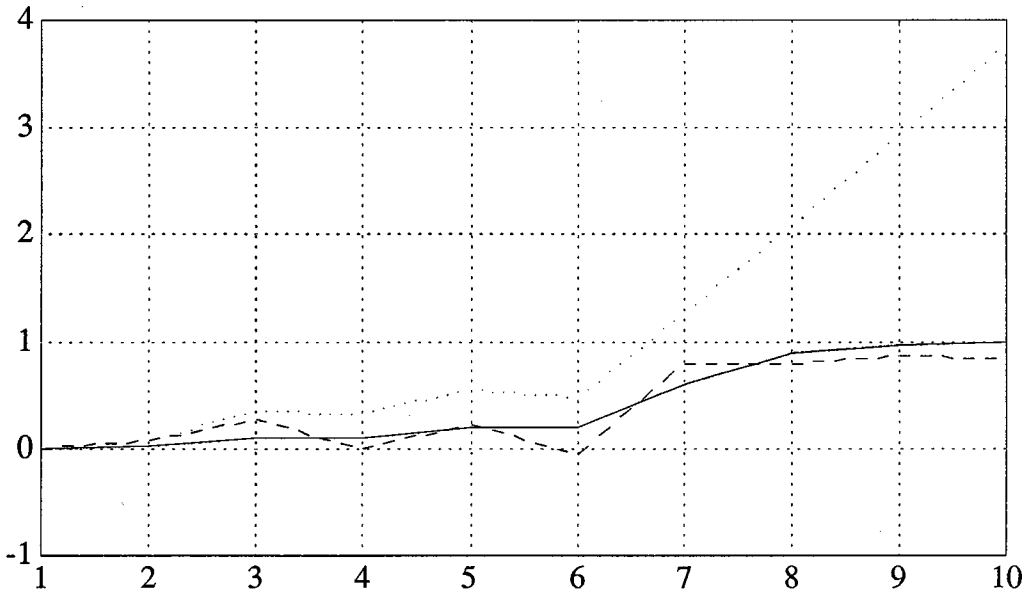

Figure 35. Recognition result with a typical reverse Y-pattern noisy path.

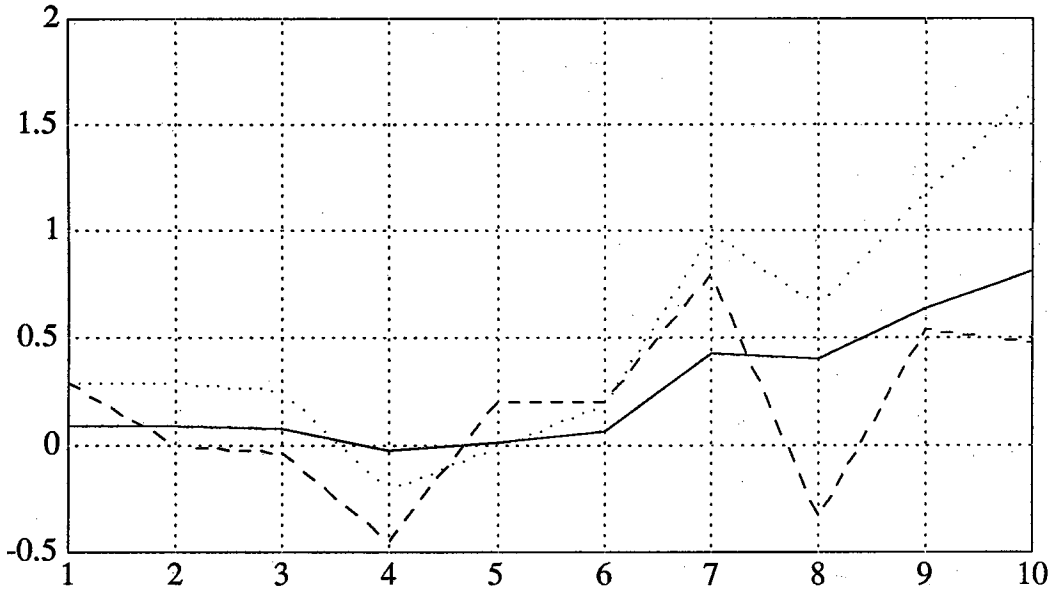

Figure 36. Recognition result with a noisy reverse Y-pattern. At time step 5, the cumulative difference is negative, yet due to the memory property of the hystery unit, its output is positive at time step 5.

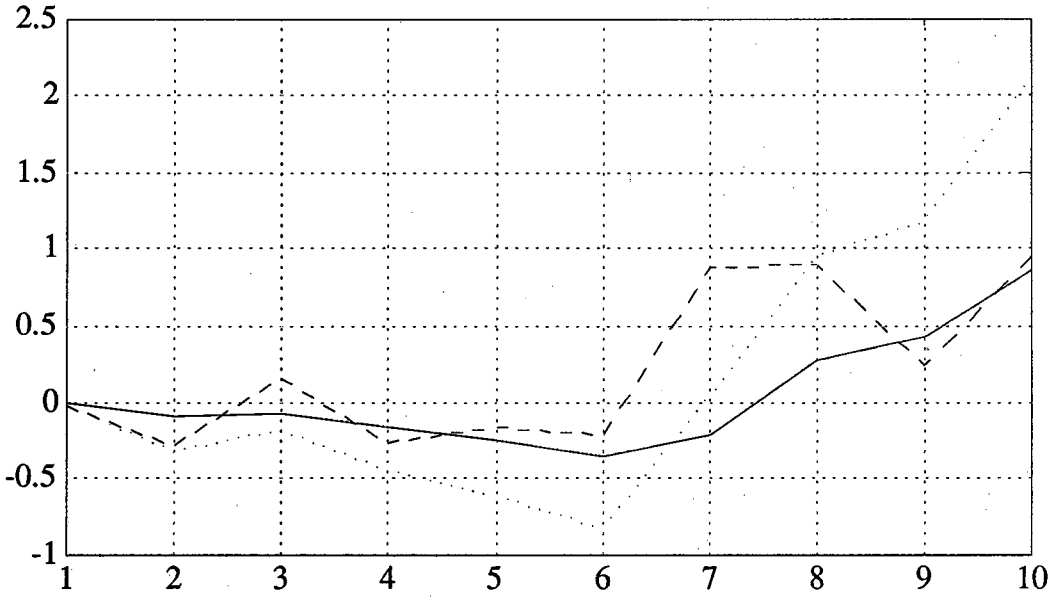

Figure 37. Recognition result with a noisy reverse Y-pattern path. At time step 7, evidence from the MIND unit drives the cumulative score positive, but due to the memory property of the hystery unit, its output is still negative at time step 7. Further correct MIND unit classifications give correct hystery unit output.

Figures 35, 36, and 37 show the reverse Y-patterns corresponding to those of Figures 32, 33, and 34. Figure 35 is typical, where the output of the hystery unit is not high when the evidence over the other path is not large. When the paths split beginning at time step seven, the gathered evidence begin to drive the hystery unit output close to 1.

In Figure 36, there is a subtle point at time step 5. Upon close examination, the cumulative score is negative, while the hystery unit output is positive. This means that the hystery unit has a memory of the past classification, as can be seen from time steps 1, 2, and 3.

Such a phenomenon is even more noticeable in Figure 37. For time steps 1 through 6, the cumulative score is negative. The hystery unit output is biased in the wrong direction (negative). At time step 7, where the cumulative score becomes positive, the hystery unit output still has a substantial negative magnitude. Here the two reversed Y-patterns split. More correct information provided by the MIND unit eventually drives the hystery unit to a correct classification.

The above observations can also be obtained from the output of the hystery unit using the X-patterns as inputs. The hystery unit gives a positive output for all 9 noisy patterns, and for both paths of the X-patterns. To increase the difficulty of the problem, the X-patterns are shortened by removing the first 3 time steps. For the first 3 time steps, the paths are widely separated. Although the noise variance is high at the beginning, the one standard deviation regions are not overlapped. (Figure 29.) By starting from the fourth time step where the one standard regions begin to overlap, the difficulty is increased. Yet the hystery unit still gives correct results to these shortened patterns.

Concluding Remarks

In this paper, several models of short term memory for the neural network unit architecture are proposed. They are inspired by the habituation and sensitization effects in neurons. Magnetic hysteresis serves as a guide in the development of these models. Several measures of memory are introduced. The hystery unit, which is a model solving two differential equations, is studied in

detail. Two theorems describing the convergence behavior of the hystery unit are proposed and proved. A conjecture is made about the full memory of the hystery unit. The above is observed for bipolar sequences of length 10. Changing the step size changes the distribution of the hystery unit output. By decreasing the step size for long sequences, the output would not be squashed close to +1 or -1. The distinct memories or outputs are attributed to a sorting behavior observed in bipolar input sequences. A mathematical argument contributes the sorting behavior to the nonlinearity of the hystery unit. An application of the hystery unit to spatiotemporal pattern classification demonstrates its operation.

In order to create a better model of the brain, it is necessary to study and learn from the neuron. The future research direction includes an experiment with a real neuron, and compare it the hystery unit's input/output behavior. Also, it is known that a real neuron would behave differently to input signals of different frequencies, whereas the hystery unit's response is frequency independent. A better model would incorporate a frequency dependent component. By using a leaky integrator instead of an accumulator, the neuron membrane's integrating effect can be modeled. This would also introduce frequency dependency. The time constant of the integrator may be obtained from experiments with the neuron membrane.

An automatic reset mechanism would be desirable in resetting the hystery unit in the spatiotemporal recognition task. Recent experiments show that the amplitude of a small amount of input noise regulates the speed of reset of the hystery unit. An external resetting device is not required.

It is mentioned in the introduction that changing a sign of a single parameter would produce an entirely different model of short term memory and learning. By changing the signs of other parameters, a wide variety of different memory models with different characteristics may be created. Moreover, interesting aggregate behaviors may be obtained by building networks of different short term memory units. For example, two hystery units with reciprocal inhibitory connections can be either oscillatory or stable. The latest developments mentioned above will be reported in a forthcoming article.

References

Several books listed below on magnetism and neurobiology have been used in the course of model development [2, 3, 4, 5, 7, 8]. In particular, Bozorth [1] provides a fairly comprehensive documentation of recordings of magnetic materials. Groves and Rebec [6] give an introduction to the neural correlates of learning and memory (chapter 14, p. 446). Shepherd [10] gives a more in depth view of the habituation and sensitation process (habituation, p. 558; sensitization, p. 591). Purves and Lichtman [9] look at learning and memory in light of the modification of central synaptic functions in invertebrates, especially in *Aplysia californica* (chapter 13, p. 317).

[1] R. M. Bozorth, *Ferromagnetism,* Van Nostrand, New York, 1951.

[2] F. Brailsford, *Magnetic Materials, 3rd. Edition,* Wiley, New York, 1960.

[3] C.-W. Chen, *Magnetism and Metallurgy of Soft Magnetic Materials,* North-Holland, Amsterdam, New York, 1977.

[4] S. Chikazumi, *Physics of Magnetism,* Wiley, New York, 1964.

[5] D. J. Craik, *Structure and Properties of Magnetic Materials,* Pion, London, 1971.

[6] P. M. Groves and G. V. Rebec, *Introduction to Biological Psychology, 3rd Edition,* Wm. C. Brown Publishers, Dubuque, Iowa, 1988.

[7] W. H. Hayt, Jr., *Engineering Electromagnetics, 5th Edition,* McGraw-Hill, New York, 1988.

[8] A. H. Morrish, *The Physical Properties of Magnetism,* Wiley, New York, 1965.

[9] D. Purves and J. W. Lichtman, *Principles of Neural Development,* Sinauer Associates Inc. Publishers, Sunderland, Massachusetts, 1985.

[10] G. M. Shepherd, *Neurobiology, 2nd Edition,* Oxford University Press, New York, 1988.

Acknowledgements: The authors would like to thank Craig Codrington for reviewing this manuscript.